Differential expression and novel permeability properties of three aquaporin 8 paralogs from seawater-challenged Atlantic salmon smolts

Morten B. Engelund[1]*, François Chauvigné[2], Birgitte Mønster Christensen[3], Roderick Nigel Finn[4,5], Joan Cerdà[2] and Steffen S. Madsen[1]

[1]Institute of Biology, University of Southern Denmark, Odense, Denmark
[2]Institut de Recerca i Tecnologia Agroalimentàries (IRTA) – Institut de Ciències del Mar, Consejo Superior de Investigaciones Científicas (CSIC), Barcelona, Spain
[3] Department of Biomedicine, Aarhus University, Aarhus, Denmark.
[4] Department of Biology, Bergen High Technology Centre, University of Bergen, Bergen, Norway
[5] Institute of Marine Research, Nordnes, Bergen, Norway

* Correspondence:
Morten Buch Engelund
Institute of Biology
University of Southern Denmark
Campusvej 55
DK-5230 Odense M
Denmark
mengelund@biology.sdu.dk

Running title: Aquaporin 8 paralogs in Atlantic salmon

Key words: aquaporin, evolution, osmoregulation, salmon, intestine, neofunctionalization

Abstract

Aquaporins may facilitate transepithelial water absorption in the intestine of seawater (SW) acclimated fish. Here we have characterized three full-length *aqp8* paralogs from Atlantic salmon (*Salmo salar*). Bayesian inference revealed that each paralog is a representative of the three major classes of *aqp8aa*, *aqp8ab* and *aqp8b* genes found in other teleosts. The permeability properties were studied by heterologous expression in *Xenopus laevis* oocytes, and the expression levels examined by qPCR, immunofluorescence and immunoelectron microscopy, and immunoblotting of membrane fractions from intestines of SW challenged smolts. All three Aqp8 paralogs were permeable to water and urea, whereas Aqp8ab and -8b were, surprisingly, also permeable to glycerol. The mRNA tissue distribution of each paralog was distinct although some tissues, such as the intestine showed redundant expression of more than one paralog. Immunofluorescence microscopy localized Aqp8aa(1+2) to intracellular compartments of the liver and intestine, and Aqp8ab and Aqp8b to apical plasma membrane domains of the intestinal epithelium, with Aqp8b also in goblet cells. In a control experiment with rainbow trout, immunoelectron microscopy confirmed abundant labeling of Aqp8ab and -8b at apical plasma membranes of enterocytes in the middle intestine and also in subapical vesicular structures. During SW-challenge, Aqp8ab showed significantly increased levels of protein expression in plasma membrane enriched fractions of the intestine. These data indicate that the Atlantic salmon Aqp8 paralogs have neofunctionalized on a transcriptional as well as on a functional level, and that Aqp8ab may play a central role in the intestinal transcellular uptake of water during SW acclimation.

Introduction

The Atlantic salmon (*Salmo salar*) is a euryhaline teleost with an anadromous life cycle during which it periodically inhabits freshwater (FW) as well as seawater (SW) environments. The internal osmolarity is maintained at approximately one third of full strength SW irrespective of the environment and thus there are strong hyperosmotic gradients with respect to FW (~1mOsm) and hyposmotic gradients with respect to SW (~1000 mOsm) (Evans et al., 2005). In FW, ions are lost to the environment by diffusion and are replaced by active absorption in the gill (Evans et al., 2005; Hwang et al., 2011) and through extraction of solutes from food particles in the intestine (Buddington and Diamond, 1987; Sundell et al., 2003). Excess water is excreted by the kidney and valuable solutes and ions are reabsorbed by the proximal and distal segments of the nephron (Beyenbach, 2004; McDonald, 2007). In SW, fluxes of ions and water are reversed. To compensate for such water loss, salmon begin drinking shortly after transfer to SW (Smith, 1932; Usher et al., 1988) and the ingested water is absorbed passively in concert with ions during passage through the gastrointestinal tract (Ando et al., 2003; Sundell & Sundh, 2012; Wood & Grosell, 2012). Excess ions are actively excreted over the gill, predominately through transcellular and paracellular routes in association with ionocytes in the gill filament (Karnaky, 1986; Hiroi et al., 2005; Tipsmark et al., 2008). Divalent ions are excreted by the kidney and intestine and an overall decrease in glomerular filtration rate (GFR) occurs in order to conserve water (Brown et al., 1978; 1980). Important water fluxes also occur in other tissues such as the liver and gall bladder during the formation of bile (Grosell et al., 2000) or in marine teleost oocytes undergoing meiotic maturation (e.g. Fabra et al., 2005; 2006; Zapater et al., 2011).

Recent studies have highlighted an important physiological role of transmembrane water channels (aquaporins) that transport water and small, noncharged solutes such as urea and glycerol for the maintenance of fluid homeostasis in fishes exposed to FW or SW environments (reviewed by Cerdà & Finn, 2010; Sundell & Sundh, 2012). Compared to mammals, however, teleosts have been shown to encode duplicate copies of most aquaporin orthologs, but up to three copies of the *aqp8* gene, consistent with both tandem and genomic duplication events early in the evolution of this lineage (Cerdà & Finn, 2010; Tingaud-Sequeira et al., 2010; Finn & Cerdà, 2011). Within some families of teleosts such as Salmonidae, yet another genome duplication is known to have occurred (Davidson et al., 2010; Moghadam et al., 2011), making it a cumbersome task to characterize all existing paralogs even for one species.

To date the piscine aquaporin superfamily has only been characterized in the diploid zebrafish (*Danio rerio*) (Tingaud-Sequeira et al., 2010), while other species of teleost have been examined with respect to basal expression patterns of selected aquaporins within osmoregulatory tissues (Cutler & Cramb, 2002; Lignot et al., 2002; Martinez et al, 2005a,b; Raldúa et al., 2008; Tingaud-Sequeira et al., 2010, Tipsmark et al. 2010; Madsen et al., 2011). Although there is some consensus on the expression pattern of each paralog, there is emerging evidence that even closely related aquaporins, such as the tandemly duplicated *aqp1aa* and *aqp1ab* genes and alternatively duplicated *aqp8* paralogs, have neofunctionalized in relation to their regulation and function (Martinez et al., 2005a,b; Tipsmark et al., 2010, Madsen et al., 2011, Finn & Cerdà, 2011; Zapater et al., 2011). In the stenohaline FW zebrafish, *aqp8* is present as three paralogs (*aqp8aa*, *-8ab* and *-8b*) and fragments of each have been found in a partial transcriptome (EST library) of the Atlantic salmon (Tingaud-Sequeira et al., 2010; Cerdà & Finn, 2010; Engelund and Madsen, 2011). In mammals, such as rats, only one AQP8 is expressed which is found in the proximal kidney tubules, hepatocytes, testes, salivary gland and intestine (Elkjær et al., 2001). In teleosts, such as the European eel (*Anguilla anguilla*), Japanese eel (*Anguilla japonica*), zebrafish and Atlantic salmon, several *aqp8* transcripts have been located in some of the same tissues although each paralog showed a distinct tissue mRNA expression pattern (Cutler et al., 2009; Kim et al., 2010; Tingaud-Sequeira et al., 2010; Tipsmark et al., 2010). Due to the extra round of genome duplication in salmonids, more *aqp8s* may exist in this species than in zebrafish and this study probably does not reveal the full complement of *aqp8*s in Atlantic salmon. Specifically, an extra *aqp8aa* was uncovered based on preliminary data from the Atlantic salmon genome during this study. These two paralogs, *aqp8aa1* and *aqp8aa2* are 92 % identical on a nucleotide level and share 91 % identical amino acid residues. Once the genome is published, more paralogs might be uncovered contributing to the evidence of the extra round of genome duplication in salmonids. However, the focus of this study is representatives of the three main types of *aqp8*, which are known from the comprehensive studies on zebrafish (Tingaud-Sequeira et al., 2010; Cerda & Finn, 2010) in order to uncover if neofunctionalization of these paralogs were important for regulation of water balance.

During SW acclimation, Atlantic salmon *aqp8ab* mRNA is strongly upregulated in intestinal segments indicating a possible role for this paralog in water balance (Tipsmark et al 2010). Similar results were found for European and Japanese eels, where SW acclimated animals showed higher levels of *aqp8* mRNA in the intestine (Cutler et al., 2009; Kim et al., 2010). The involvement of

Aqp8 in the SW acclimation of Atlantic salmon was further supported by recent work in our laboratory where a homologous antibody detected Aqp8ab in the brush borders and lateral membranes of enterocytes (Madsen et al., 2011).

In the present study, we set out to expand the knowledge of Aqp8 biology in Atlantic salmon by investigating the tissue distribution of *aqp8* mRNAs and determine the cellular locations of Aqp8aa(1+2), -8ab and -8b proteins using homologous antibodies. We additionally examined the protein expression of Aqp8ab and Aqp8b in two intestinal segments to establish whether the suggested role of Aqp8ab during SW acclimation (Tipsmark et al., 2010) could be confirmed at the protein level and if differences existed between the paralogs. The permeability properties of the three paralogs were investigated in *X. laevis* oocytes in order to reveal potential neofunctionalization, which could shed light on whether tissue specific expression patterns are linked to functional diversity.

Materials and methods

Animals

Atlantic salmon presmolts were obtained from the Danish Centre for Wild Salmon (Randers, Denmark). The fish spent the spring in outdoor tanks under natural light and temperature conditions and were moved to the university campus in June 2010 to an indoor aquarium with biofiltered recirculated freshwater where a photoperiod of 12h: light 12h: dark and a constant temperature of 14^{o}C was upheld. In September 2010, a group of fish was moved to a tank containing artificial 25 ppt seawater (Red sea salt, Eliat, Israel) where they remained for at least three weeks prior to sampling. The fish were fed *ad libitum* using commercial fish pellets and food was generally withheld 3 days before an experiment. Fish were anesthetized with 0.2 ppt phenoxy ethanol and euthanized by cutting the spinal cord and pithing the brain before samples for RNA analysis and histology were taken. Long term SW- or FW-acclimated salmon were then used for the tissue screening of *aqp8* transcripts while intestine and liver from SW acclimated salmon were used for immunofluorescence microscopy. Middle intestine from long term SW acclimated rainbow trout (*Oncorhynchus mykiss*), (~ 40g) obtained from Lihme Dambrug, (Randbøl, Denmark) was used for immunoelectron microscopy. All experimental procedures were approved by the Danish Animal Experiments Inspectorate in accordance with the European convention for the protection of vertebrate animals used for experiments and other scientific purposes (#86/609/EØF).

144

145 *Seawater acclimation experiment*

146 In late April 2012, one year-old smolts (20 – 30 g, N=100) were transferred to a tank containing 25
147 ppt SW at the Danish Centre for Wild Salmon and ten fish were anesthetized and sampled as
148 described above following 6 hrs, 24 hrs, 72 hrs and 168 hrs in SW. At the same time, a control
149 group of smolts (N=100) were sham-transferred to a tank containing FW and sampled accordingly.
150 Ten smolts were sampled prior to sham or SW transfer to represent time point 0 hrs.

151

152 *Cloning of Atlantic salmon aquaporins aqp8aa1, aqp8ab and aqp8b*

153 Full-length sequences of Atlantic salmon *aqp8* mRNAs were cloned using RNA from the middle
154 intestine for *aqp8ab* and *aqp8b* and from the liver for *aqp8aa1*. RNA was purified using TRIsure™
155 (DNA Technology, Risskov, Denmark) according to the manufacturer's instructions. cDNA
156 synthesis was performed with an oligo $dT_{(15)}$ primer using DyNAmo™ cDNA synthesis kit
157 (Thermo Scientific, Søborg, Denmark) according to the manufacturer's instructions. The full
158 mRNA sequence for *aqp8ab* and *aqp8b* was readily available from the EST database for Atlantic
159 salmon at www.ncbi.nlm.nih.gov based on previous annotations (See legend, Table 1) (Cerdà and
160 Finn, 2010; Tipsmark et al., 2010). The full *aqp8ab* cDNA was amplified in one PCR reaction
161 using the cloning primers stated in Table 1. PCR conditions were an initial denaturing for 3 min at
162 94°C followed by 35 cycles of 94°C for 45 sec, 59°C for 45 sec and 72°C for 1 min ending with a
163 final elongation at 72°C for 12 min. Cloning primers included restriction enzyme sequences for Bgl
164 II and Eco RV in the 5' and 3' end respectively. The *aqp8b* cDNA was obtained using a nested PCR
165 design. First, 35 cycles of PCR as explained above was performed with primers aligning outside the
166 coding sequence (Table 1). This was followed by 15 cycles of PCR using cloning primers (Table 1)
167 with a slight increase in annealing temperature of the PCR reaction to 61°C. The *aqp8aa1* cDNA
168 was obtained by PCR using primers aligning to the 3'UTR of rainbow trout (*Oncorhynchus mykiss*)
169 *aqp8aa* and the 5'UTR of the Atlantic salmon *aqp8aa1*. After the initial PCR reaction using these
170 primers another PCR reaction was performed for 35 cycles using cloning primers (Table 1).
171 Annealing temperature was 61°C and the other parameters of the PCR reaction were the same as
172 described above. The transcripts were ligated into the pT7Ts oocyte expression vector, which was
173 then used as a template for *in vitro* transcription (see below). Each paralog was sequenced in both
174 directions to ensure a complete cDNA.

175

Phylogenetic analysis

Deduced amino acid sequences of the isolated Atlantic salmon mRNAs were aligned with other teleost Aqp8 orthologs retrieved from public databases (Ensembl v70 and GenBank) using the MAFFT (v7.017b) and T-Coffee (9.03.r1318) software packages (Notredame et al., 2000; Katoh & Toh, 2008). Amino acid alignments were converted to codon alignments using Pal2Nal (Suyama et al., 2006) and molecular phylogenies inferred using Bayesian (Mr Bayes v3.2.0; 5 million generations; Ronquist & Huelsenbeck, 2003) and maximum likelihood (PAUP v4b10-x86-macosx; Swafford, 2002) protocols as described previously (Zapater et al., 2011, 2013).

Water permeability of X. laevis oocyte expressing salmon aquaporin 8's

Atlantic salmon *aqp8* cDNAs were cloned into the *Eco*RV/BglII sites of the oocyte expression vector pT7Ts (Deen et al. 1994). The cRNAs were synthesized as described (Deen et al. 1994) and microinjected into *X. laevis* stage V–VI oocytes. Oocytes were maintained in 200 mOsm modified Barts Solution (MBS, in mmol L^{-1} 0.33 $Ca(NO_3)_2$, 0.4 $CaCl_2$, 88 NaCl, 1 KCl, 2.4 $NaHCO_3$, 0.82 $MgSO_4$, 10 4-(2-hydroxyethyl)-1-piperazine-ethanesulfonic acid (HEPES) pH 7.5) and were injected with 50 nl of water containing 1-10 ng cRNA of one of the three salmon aquaporin 8 paralogs. Control oocytes were not injected since injection does not affect the water permeability of oocytes (data not shown). After 24 hours, the oocytes were manually defolliculated and following another 24 hours, the water permeability of the oocytes was determined by measuring the time-course changes in the relative volume of the oocytes when incubated in 10 fold diluted MBS. The volume of the oocyte was determined by recording the maximal surface area of the oocyte every 2 seconds using time lapse microscopy. Assuming that the oocyte is a perfect sphere, the relative volume change can then be calculated from the obtained surface area. The osmotic water permeability (P_f) was determined according to the following equation: $P_f = \frac{V_0\left[\frac{d(V/V_0)}{dt}\right]}{S \cdot V_w (Osm_{in} - Osm_{out})}$

Where $\left[\frac{d(V/V_0)}{dt}\right]$ is the relative volume change of the oocyte with time incubated in the diluted media, S is the surface area of the oocyte and V_w is the molar volume of water (18 cm^3). Inhibition of water transport by mercury was investigated by incubating oocytes in MBS containing 0.1 mM $HgCl_2$ for 15 min prior to measurement. Recovery of water transport was measured by transferring $HgCl_2$ incubated oocytes through two washes with clean MBS to a solution of MBS with 5 mM mercaptoethanol for 15 min prior to measurement.

206

207 *Urea and glycerol uptake of X. laevis oocytes expressing salmon aqp8's*

208 Oocytes were injected with 50 nl of water or water containing 15ng cRNA of a salmon *aqp8*
209 paralog. Groups of 10 oocytes were incubated in 200 µl of MBS containing 20 µCi of
210 [1,2,3-^{3}H]glycerol (50 Ci/mmol) or [^{14}C]urea (58 mCi/mmol) at room temperature. Cold solute was
211 added to give 1 mM final concentration. After 10 min, which included zero time for subtraction of
212 the signal from externally bound solute, oocytes were washed rapidly in ice-cold MBS three times,
213 and individual oocytes were then dissolved in 5% Sodium-dodecyl-sulfate (SDS) for scintillation
214 counting.

215

216 *Tissue screening of salmon aquaporin 8 paralogs*

217 Expression of salmon aquaporin mRNA in various tissues has previously been reported for *aqp8aa*
218 and *aqp8ab* (Tipsmark et al., 2010) but was repeated in the current experiment for comparison with
219 *aqp8b*. Total RNA was extracted from 14 different tissues of four Atlantic salmon as explained
220 above. The RNA was subjected to DNAse treatment with RQ1 RNAse-Free DNAse (Promega
221 Biotech AB, Stockholm, Sweden) according to manufacturer's protocol. Synthesis of cDNA took
222 place with the use of the High Capacity cDNA Reverse Transcription Kit (Applied Biosystems,
223 Carlsbad, CA, USA). Real time quantitative PCR (qPCR) was performed on a Mx3000p instrument
224 (Stratagene, La Jolla, CA, USA) using the primers stated in Table 1. Primers for *aqp8aa* and
225 *aqp8ab* were the same as reported in Tipsmark et al (2010) and primers for *aqp8b* were designed
226 using Primer 3 software (Rozen and Skaletsky, 2000). Preliminary data from the Atlantic salmon
227 genome became available during the publication process of this study and showed that two *aqp8aa*
228 paralogs (*aqp8aa1* and *aqp8aa2*) exist and the primers designed for qPCR are unable to distinguish
229 between these two paralogs as they are 92 % identical in the coding sequence. Results for this
230 paralog are therefore named *aqp8aa(1+2)*. BlastN of each primer pair against the cloned sequence
231 of each paralog showed no similarity other than against the paralog for which the primers were
232 designed. For each paralog, the PCR product was validated by agarose gel electrophoresis and
233 melting curve analysis. A two-step standard qPCR reaction (95°C for 30 sec and 60°C for 1min for
234 40 cycles) was performed using SYBR Green Jumpstart Taq Readymix (Sigma-Aldrich, St. Louis,
235 MO, USA). Total reaction volume was 25µl and primers were used at a concentration of 150 nM.
236 The relative expression of the *aqp8* paralogs was normalized to the expression of elongation factor
237 1a (*ef1a*) according to Olsvik et al. (2005). Efficiency of amplification (E_a) for each set of primers

was calculated by standard curve analysis of increasing diluted solutions of cDNA according to Pfaffl (2001). Normalized expression of each paralog was then calculated as:

$$C_n = \left(1 + E_{a(\text{target})}\right)^{-Ct(\text{target})} / \left(1 + E_{a(\text{EF1a})}\right)^{-Ct(\text{EF1a})}$$

Where Ct is the threshold cycle and Cn is the relative copy number of the target gene.

Primary antibodies

The homologous polyclonal antibodies used in this study were raised in rabbits by BioGenes, (Berlin, Germany). A synthetic peptide corresponding to a N-terminal epitope (Aqp8aa1: CFTVAGADTGDSGPG-amide; Aqp8ab: CGHSTLMSGTKKPTP-amide; Aqp8b: CMASDSKKAPVKPPN-amide) for each paralog was used to immunize the rabbits and the collected antisera was affinity purified against the antigenic peptide by BioGenes (Aqp8ab, Madsen et al., 2011) or by use of the SulfoLink$^{(R)}$ Immobilization Kit for Peptides (Aqpp8aa1 and Aqp8b, current study) (Thermo Scientific, Waltham, MA, USA) according to the manufacturer's instructions. For immunofluorescence and immunoelectron microscopy, serum was used. Cross reactivity of each antibody toward the other paralogs was minimal as shown by incubation of each antibody against a crude membrane fraction from *X. laevis* oocytes expressing each of the three paralogs (Fig.2C). The antibody developed against Aqp8aa1shares 12 out of 15 amino acids with the preliminary Aqp8aa2 sequence, so the antibody may very well bind to both proteins. Preadsorption of the antibodies with up to 100 fold molar excess of the respective antigenic peptide abolished binding of the antibody to Western blots of oocyte membrane fractions expressing each aquaporin or homogenates from pyloric caeca or liver (data not shown, Aqp8ab antibody validated in Madsen et al. (2011)).

Immunoblotting of oocytes and tissues

Total membrane fractions from *X. laevis* oocytes injected with 15 ng of *aqp8aa1*, *aqp8ab* or *aqp8b* cRNA were prepared according to Kamsteeg & Deen (2001). Ten oocytes, frozen in liquid N_2, were homogenized in HbA buffer (in mmol L^{-1} 20 Tris-HCl (pH 7.4), 5 $MgCl_2$, 5 NaH_2PO_4, 1 ethylenediaminetetraacetic acid (EDTA), 80 Sucrose and 1% v/v of a protease inhibitor cocktail (P8340, Sigma-Aldrich)) using a P200 pipette and subsequently centrifuged for 5 min at 200 x *g* at 4°C. The supernatant from this step was centrifuged again under the same conditions and the resulting supernatant was centrifuged for 20 min at 20,000 x *g* to pellet a total membrane

preparation. The pellet was resuspended in 1x NuPAGE LDS sample buffer (Invitrogen, Carlsbad, CA, USA) in a volume of 0.33 oocyte/µl.

Liver or intestinal tissue were homogenized in SEI buffer pH 7.3 (in mmol L^{-1} 300 sucrose, 20 Na_2EDTA, 50 imidazole, 1% v/v of a protease inhibitor cocktail (P8340, Sigma-Aldrich)) with a tight fitting glass mortar and pestle, followed by centrifugation at 2000 x *g* for 10 min at 4°C. The supernatant was then recentrifuged for 30 min at 50.000 x *g* to pellet an enriched plasma membrane fraction. The pellet was resuspended in 1x NuPAGE LDS sample buffer in a concentration of 5 µg/µl. SDS PAGE and electro-blotting was performed using the NuPAGE system (Invitrogen) according to the manufacturer's instructions. 50 µg of liver or intestinal protein or 3.3 oocytes was loaded per lane and separated by 200 V for 35 min using a 2-(N-morpholino)ethanesulfonic acid (MES) running buffer (Invitrogen). Proteins were then blotted onto a nitrocellulose or PVDF membrane using a tris-glycine transfer buffer (in mmol L^{-1} 7.5 Tris, 60 glycine 20% v/v methanol) for two hours at a constant 25 V. Membranes were blocked for one hour at room temperature in 2% bovine serum albumin (BSA) in tris-buffered saline containing Tween 20 (TBS-T; in mmol L^{-1} 20 Tris, 140 NaCl, 1% Tween 20). Primary antibodies (Rabbit IgG anti Aqp8aa1, Aqp8ab or Aqp8b, (all 2.5µg/ml)) and mouse anti β-actin (0.25 µg/ml, Abcam, Cambridge, UK) were diluted in TBS-T containing 2 % BSA and incubated overnight at 4°C. Membranes were washed four times 5 min in TBS-T and incubated in TBS-T and 2% BSA with goat-anti rabbit and goat-anti mouse IgG secondary antibodies conjugated to the fluorophores Cy5 and Cy3 respectively (Invitrogen) for 1 hr at room temperature. The membrane was then washed four more times in TBS-T and allowed to dry overnight before being scanned with a Typhoon Trio Variable mode Imager (GE Healthcare, Little Chalfont, UK). Relative measurements of protein abundance were performed with the ImageJ gel analyzer tool (http://rsbweb.nih.gov/ij/docs/menus/analyze.html#gels) and β-actin was used for normalization of protein abundance.

Immunofluorescence of oocytes and tissue sections

Tissues were dissected out of the SW acclimated fish and immediately fixed in 4% paraformaldehyde (4% PFA, 0.9% NaCl, 5 mmol L^{-1} NaH_2PO_4, pH 7.4) overnight at 4°C. They were then washed repeatedly in 70% EtOH before being transferred through increasing concentrations of EtOH to xylene and embedded in paraffin blocks. Five µm thick tissue sections were cut and heated at 55°C (oocytes at 37°C overnight) for two hours before being hydrated through decreasing concentrations of EtOH. Tissue sections were demasked by boiling in Tris

EDTA buffer (in mmol $^{L-1}$ 10 Tris, 1 EDTA, 0.05% Tween-20) for 10 minutes and left to cool for 30 min at room temperature. Oocytes did not undergo antigen retrieval. After one wash in PBS (in mmol L^{-1} 137 NaCl, 2.7 KCl, 1.5 KH_2PO_4, 4.3 Na_2HPO_4, pH 7.3), sections were blocked for 30 min in PBS-T (PBS, 0.05% Tween-20) containing 5 % normal goat serum and 0.1 % BSA. They were then incubated overnight at 4°C with a cocktail of primary antibodies against one of the salmon Aqp8 paralogs (Rabbit IgG 1-5µg/ml) and against the alpha subunit of the Na^+, K^+ ATPase (mouse IgG α5 0.5µg/ml; The Developmental Studies Hybridoma Bank developed under auspices of the National Institute of Child Health Development and maintained by The University of Iowa, Department of Biological Sciences, Iowa City, IA, USA). After four washes in PBS-T, sections were incubated for 1 hr at room temperature with secondary antibodies (4 µg/ml) goat anti mouse IgG Alexa Fluor$^{(R)}$ 568 and goat anti rabbit IgG Oregon Green$^{(R)}$ 488 (Invitrogen). Sections were washed four times in PBS-T and in some cases after the second wash incubated for 5 min with 0.1 µg/ml of 4', 6-diamidino-2-phenylindole (DAPI) in PBS to stain the nuclei of the cells. Sections were then washed twice in PBS-T followed by a wash in dH_2O before being allowed to dry. Cover slips were mounted on the slides with ProLong Gold antifade reagent (Invitrogen). Stained tissues were inspected with a Leica HC microscope (Leica Microsystems A/S, Ballerup, Denmark) and representative pictures were obtained with a Leica DC200 camera. Confocal microscopy was performed with a Zeiss LSM510 META confocal microscope (Carl Zeiss Inc.).

Immunoelectron microscopy

Intestinal samples were isolated from three rainbow trouts and fixed in 4% neutral buffered PFA overnight at 4°C. Tissue blocks of the middle intestine were dissected from the remaining intestine and infiltrated for 2 hr with 2.3 M sucrose in 10 mM PBS, mounted on holders and rapidly frozen in liquid nitrogen. Ultrathin cryosections (80 nm) were cut on an ultra-cryomicrotome (Reichert Ultracut S, Leica, Microsystems, Vienna, Austria) and pre-incubated in 10 mM PBS with 0.1% skimmed milk powder and 50 mM glycine. The sections were incubated overnight at 4° C with Aqp8ab or Aqp8b serum diluted in 10 mM PBS containing 0.1% skimmed milk powder. The primary antibodies were visualized by incubation for 1 hr at room temperature with secondary goat anti-rabbit IgG conjugated to 10 nm colloidal gold particles (GAR.EM10, Bio-Cell Research Laboratories, Cardiff, UK; dilution: 1:50) diluted in PBS with 0.1% skimmed milk powder, 0.06%

polyethyleneglycol and 1% fish gelatin. Electron micrographs were taken on a Morgagni 268D FEI electron microscope (FEI, the Netherlands).

Statistics

All statistical comparisons were performed using GraphPad Prism v5.02 (GraphPad Software, La Jolla, CA, USA). Data were analyzed via one-way or two-way ANOVA where appropriate followed by Tukey's (one way ANOVA) or Bonferroni's (two way ANOA) multiple comparisons *post hoc* test if they showed a Gaussian distribution. If transformation of the data did not result in a Gaussian distribution, a non parametric Kruskal-Wallis test was performed with a Dunn's *post hoc* test to compare between data sets. Data were adjusted for outliers using Grubbs' test. Values are reported as means ± SEM.

Results

Cloning and phylogeny of Atlantic salmon aqp8 paralogs

Three full-length cDNAs ranging in length from 798 – 858 bp were isolated from intestinal and hepatic tissues of Atlantic salmon. Each cDNA contained open reading frames (ORFs) of 780 or 798 bp, and encoded proteins of 259 or 265 amino acids, respectively. Alignment of the deduced amino acids and Bayesian inference of the codons and proteins in relation to other teleost *aqp8* orthologs revealed that each Atlantic salmon paralog clustered as one of the three major classes of *aqp8* found in zebrafish (Fig. 1; See supplementary Table S1 for accession numbers). Within each subcluster, however, the topology of transcripts and proteins closely reflected the expected phylogenetic rank, where the Atlantic salmon sequences clustered together with other salmonids. These data revealed that two *aqp8aa* genes appear to exist in Atlantic salmon which are 92 % identical based on preliminary data from the salmon genome for *aqp8aa2*. The longest sequence was *aqp8aa1* (Acc# KC626878), which encoded the 265 amino acid protein with an estimated molecular mass of 27.1 kDa, while the two shorter ORFs encoded the Aqp8ab (Acc# KC626879) and Aqp8b (Acc# KC626880) proteins with estimated molecular masses of 27.5 and 27.3 kDa, respectively. Maximum likelihood analyses of the codon alignment confirmed the topology determined via Bayesian inference (data not shown). Comparison of the three Atlantic salmon and zebrafish Aqp8 orthologs showed high rates of amino acid substitution (37 - 39%) for the Aqp8aa1 and Aqp8b proteins, but only 25% for the Aqp8ab proteins. As noted previously for zebrafish (Finn & Cerdà, 2011), each Atlantic salmon paralog retains a long N-terminus, a short C-terminus and the

six transmembrane-spanning domains that are typical of the aquaporin superfamily. In contrast to the Aqp8aa1 paralog, which encodes a canonical NPA motif on hemihelix 3, the Aqp8ab and Aqp8b paralogs harbor non-canonical NPP motifs in this position. Inspection of other teleost Aqp8ab orthologs revealed that each retained the NPP motif on hemihelix 3, while the Aqp8b orthologs were more variable with either a Pro in the third position as found in Atlantic salmon, a Thr in flatfishes such as Atlantic halibut (*Hippoglossus hippoglossus*) and European flounder (*Platichthys flesus*), or a Ser as found in zebrafish.

Functional characterization of salmon aquaporin 8 paralogs

Immunofluorescence microscopy, and western blotting of membrane fractions of *X. laevis* oocytes expressing the salmon Aqp8s showed that all three paralogs were translated and translocated to the oocyte plasma membrane and thus able to regulate the permeability of the oocyte (Fig. 2A,C). Accordingly, oocytes expressing Aqp8aa1, -8ab and -8b showed a ~30-, ~19- and ~17-fold increase in Pf, respectively, with respect to the control oocytes, which was inhibited with mercury and partially reversed with ß-mercaptoethanol only in the case of Aqp8ab (Fig. 2B). The three salmon Aqp8 paralogs were permeable to urea, but interestingly Aqp8ab and -8b also appeared to transport significant amounts of glycerol (Fig. 2B). The observed molecular weights of the Atlantic salmon Aqp8 paralogs in *X. laevis* oocyte membrane fractions were smaller than the theoretical estimates (Fig. 2C). However, when antibodies were used on membrane fractions from intestinal tissue, the major antigenic signal appeared at ~27-28 kDa (Fig. 3D, Aqp8ab and -8b). The antibodies detected high molecular bands >50kDa in both noninjected oocytes and oocytes injected with salmon Aqp8 cRNA, but this non-specific band was not present in intestinal samples (Fig. 2C vs. 3D). However, in intestinal samples a ~38 kDa band was often seen (Fig. 3D). When the antibodies were used for immunofluorescence on noninjected oocytes only weak autofluorescence was observed (Fig. 2A (Ctrl), representative image).

Tissue screening of salmon aquaporin 8 paralogs

The Atlantic salmon *aqp8* paralogs each had a distinct expression profile in the range of tissues examined in this study. mRNAs of *aqp8aa(1+2)* were found mainly in the liver (Fig. 3A), but also at basal levels in nearly all other tissues examined, except for the brain, which showed slightly higher expression levels. mRNAs of *aqp8ab* were expressed exclusively in the intestinal segments and the spleen (Fig. 3C), while *aqp8b* mRNAs were expressed at varying levels in all tested tissues

(Fig. 3E). The most prominent *aqp8b* expression was found in the brain, but significant expression was also detected in osmoregulatory tissues such as the esophagus, intestine, kidney and gill. When comparing two long-term SW-acclimated salmon with two FW-acclimated salmon (Fig. 3D,F) *aqp8ab* mRNA (Fig. 3D) but not *aqp8b* mRNA (Fig. 3F) tended to be higher in the intestinal tissues of SW-acclimated salmon. Protein expression levels of Aqp8ab were accordingly high for Aqp8ab in 7 day SW-acclimated fish (Fig. 3B, lane a, see also Fig. 6)) but low in sham transferred fish (Fig 3B, lane b), whereas it did not change for Aqp8b (Fig 3B, lane c,d). In the spleen there was a remarkably higher level of mRNA from both paralogs in SW- acclimated salmon even though the low n-number eliminated statistical comparisons (Fig 3D,F).

Cellular and subcellular localisation of salmon aquaporin 8 proteins

Aqp8aa(1+2) was localized in intracellular compartments of enterocytes of the middle intestine, where staining was sub-apical below the brush border (Fig. 4A, inset). Aqp8aa(1+2) was also found in hepatocytes of the salmon liver where staining appeared in a granular pattern reminiscent of cytosolic vesicles (Fig. 4B). In the intestine, Aqp8ab was abundant in the enterocyte brush border in both middle and posterior intestine with some occasional staining of the basolateral plasma membrane domains of the enterocytes where it co-localized with the alpha subunit of the Na^+, K^+ ATPase. (Fig. 4D,E; yellow staining). Aqp8b was found in the brush border membrane of the middle and posterior intestine (Fig. 4G,H). This protein was present in goblet cells of the middle intestine (Fig. 4G) but also found at subapical locations throughout the intestinal tissue (Fig. 4G,H). Pre-immune serum for each antibody showed no specific staining of the intestine but only a weak autofluorescence (Fig. 4C,F,I). To eliminate the possibility that the brush border staining observed for Aqp8ab and -8b was due to non specific binding of the primary antibody to the glycocalyx a control experiment using immunoelectron microscopy was performed on the closely related rainbow trout. Immunoelectron microscopy of the middle intestine of rainbow trout revealed abundant Aqp8ab and Aqp8b labeling of the apical plasma membrane (brush border) as well as labeling of intracellular vesicles located subapically in the enterocytes (Fig. 5A-D).

Time-course changes in protein expression of Aqp8ab and 8b in intestinal segments

The abundance of the ~28 kDa Aqp8ab protein band in intestinal tissues significantly increased in response to SW-transfer (Fig. 6A,C). Seven days after SW-transfer the abundance of Aqp8ab was significantly higher in membrane fractions from pyloric caeca and the middle intestine of SW

transferred individuals compared to sham transferred fish. There was a significant interaction between "time" and "SW" on Aqp8ab expression in both tissues tested. High proteolytic activity in samples from the posterior intestine made it impossible to probe for changes in Aqp8ab and Aqp8b protein expression in this segment. Some truncated protein fragments between 10-14 kDa were detected by the Aqp8ab antibody in some intestinal samples from both SW- and FW-acclimated fish (Fig. 6E). A reaction with the Aqp8ab antibody was also seen around 38 kDa in samples with high abundance of the 28 kDa protein possibly reflecting a glycosylated form of the aquaporin (Fig. 6E). The abundance of the ~27 kDa Aqp8b protein did not change significantly in membrane fractions from pyloric caeca or the middle intestine during seven days of SW-acclimation, and the variation in protein abundance was high in both SW-acclimated fish and sham transferred fish (Fig. 6B,C,F). Time-course changes in Aqp8aa(1+2) protein expression were not investigated because of its low abundance in membrane fractions from intestinal tissues possibly due to its intracellular localization. Hence, it was a less obvious candidate for transcellular water transport.

Discussion

AQP8 is a versatile transmembrane channel expressed in multiple tissues of different mammals where it has been suggested to be involved in the maintenance of intracellular osmotic equilibrium, transport of ammonia and small organic solutes or mitochondrial expansion during oxidative phosphorylation (Elkjær et al., 2001, Calamita et al., 2005; Saparov et al., 2007). In contrast to mammals, in which only a single *AQP8* gene is known, the multiplicity of Aqp8 paralogs in fish offers a possibility of dissecting the evolutionary form and function of a closely related set of genes. The current study adds knowledge to the puzzle of Aqp8 evolution initiated recently through studies on zebrafish (Tingaud-Sequeira et al., 2010; Cerdà & Finn, 2010; Finn & Cerdà, 2011). We extend the available information by identifying novel transport properties of two Aqp8 paralogs in Atlantic salmon and show for the first time that the expression of Aqp8ab channels, which are located in the brush border of enterocytes, is upregulated in response to SW acclimation.

Phylogenetic analysis of salmon aquaporin 8 paralogs

The Bayesian analyses clearly show that the Atlantic salmon *aqp8* paralogs isolated in the present study are representatives of the three major classes of *aqp8* genes originally identified and characterized in zebrafish (Tingaud-Sequeira et al., 2010). The present observation that the subcluster topology closely follows the phylogenetic rank of each species and that each paralog

retains conserved features, such as the canonical and non-canonical NPA motifs, is consistent with an early diversification of the *aqp8* genes during fish evolution (Cerdà & Finn, 2010; Finn & Cerdà, 2011). This became evident when the genomic synteny of the different paralogs was examined revealing that *aqp8aa* and *aqp8ab* are closely linked in distantly related teleost genomes whereas *aqp8b* is located on a different chromosome (Cerdà & Finn, 2010). The presence of a second *aqp8aa* gene reported here for Atlantic salmon is potentially consistent with the occurrence of a fourth round of genome duplication in the salmonid lineage (Moghadam et al., 2011).

Functional characteristics of salmon aquaporin 8 paralogs

The permeability properties of mammalian AQP8 has been under dispute for some years, since studies of human, rat and mouse AQP8 using *X. laevis* oocytes or reconstituted liposomes have led to different conclusions. All studies show that AQP8 is water permeable but its ability to also transport small solutes such as urea is controversial (Liu et al., 2006; Yang et al., 2006). The three salmon aquaporin paralogs were successfully translated in *X. laevis* oocytes and the protein products transported to the plasma membrane as demonstrated by Western blotting of enriched membrane fractions and immunofluorescence microscopy. All paralogs showed significant water permeability, as expected from studies performed on mammalian AQP8 channels (Liu et al., 2006; Yang et al., 2006; Saparov et al., 2007). The significant urea permeability of all three paralogs corresponds well with the fact that two out of three zebrafish paralogs (Aqp8aa and Aqp8ab, Tingaud-Sequeira et al., 2010) and the murine AQP8 ortholog (Ma et al., 1997) are also permeable to urea. Rat and human AQP8, however, seem not to be urea permeable (Liu et al., 2006). Glycerol permeability has not been reported for any vertebrate Aqp8 ortholog, but this study shows that two of the Atlantic salmon paralogs, Aqp8ab and -8b, are significantly permeable to glycerol. It is somewhat surprising that the liver paralog Aqp8aa1 did not show glycerol permeability, since glycerol metabolism in this organ is of major importance. Aqp8aa2, which was not cloned and expressed in *X. laevis* oocytes, is suspected to function similarly as Aqp8aa1 due to their high degree of identical amino acid residues. The intestinal paralog Aqp8ab showed the highest glycerol permeability, perhaps suggesting a potential role of this aquaporin in glycerol mobilization in addition to water transport.

Tissue specific expression of aqp8 paralogs

The tissue expression profile for Atlantic salmon *aqp8aa(1+2)* mRNA reported here is consistent with that of the *aqp8aa2* gene (formerly annotated as *aqp8a*,Tipsmark et al., 2010), which was highly expressed in the liver. The study by Tipsmark et al. (2010) may also have amplified *aqp8aa1* mRNA as the primers used then were the same as in the current study and they are unable to distinguish between the two paralogs. The *aqp8aa1* paralog was cloned from the liver and thus is expressed in this tissue to some degree. Due to the high similarity between the two *aqp8aa* paralogs in comparison with the other *aqp8* paralogs in salmon, one might expect them still to be expressed in the same tissues. On the other hand, as is seen with aqp8's in several teleosts, the expression patterns of the paralogs are highly dynamic and may be subjected to selection early on after a genomic duplication event. A final answer to the evolutionary kinship between aqp8aa1 and aqp8aa2 and the relative abundance of the two paralogs await further investigation which will be more interesting from an evolutionary perspective than an osmoregulatory one. The tissue expression profile of the Atlantic salmon *aqp8ab* gene is more similar to that reported for the zebrafish *aqp8ab* gene (Tingaud-Sequeira et al., 2010). The presence of *aqp8* mRNAs in intestinal segments has been observed earlier in different teleosts although the particular paralog expressed varies between species. For example, eels may express the *aqp8aa* paralog (Cutler et al., 2009; Kim et al., 2010), zebrafish expresses both the *aqp8aa* and *-8ab* paralogs (Tingaud-Sequeira et al., 2010), while Atlantic salmon expresses the *aqp8ab* and *-8b* paralogs (Tipsmark et al., 2010, and present study). In Atlantic salmon, *aqp8ab* mRNA was also present in the spleen, where its apparent upregulation in SW acclimated animals has not been reported previously. This expression must take place in the splenic tissue itself and not in the abundant blood cells, since a screening of mixed blood cells from the closely related rainbow trout did not reveal any expression of *aqp8ab* mRNA (M.B. Engelund, unpublished observations). There are as yet no other reports of Aqp8 expression in the teleost spleen. The intestinal levels of *aqp8ab* mRNA tended to be elevated in long term SW-acclimated animals which is consistent with earlier findings (Cutler et al., 2009; Kim et al., 2010; Tipsmark et al., 2010). In contrast to the tandemly duplicated *aqp8aa1* and *-8ab* transcripts, expression of *aqp8b* is more ubiquitous, with the highest expression levels occurring in the brain. The earlier study in zebrafish (Tingaud-Sequeira et al., 2010) only found expression of *aqp8b* mRNA in the brain, thus the expression of this paralog seems to be highly species specific. As noted for *aqp8ab*, there seemed to be a higher expression of *aqp8b* in the spleen upon SW acclimation, which could represent expression in blood cells or in the splenic tissue itself.

Cellular and subcellular localization of salmon aquaporin 8 proteins

Only selected tissues were investigated by immunofluorescence microscopy in this study because of our focus on the role of Aqp8 in water transport upon SW acclimation. The intracellular immunolocalization of Aqp8aa(1+2) in both the liver and intestine of Atlantic salmon resonates well with earlier findings of AQP8 in mammals. For example, vesicular localization of AQP8 has been reported in rat kidney tubules (Elkjær et al. (2001), subapical localization in the jejunum and duodenum (Elkjær et al., 2001; Laforenza et al., 2005; Tritto et al., 2007) with intracellular localization noted in colonic enterocytes and hepatocytes (Elkjær et al., 2001). The hepatic vesicular localization in rat was confirmed in studies by Garcia et al. (2001), who further demonstrated that cAMP was a strong stimulus for redistribution of the protein to the plasma membrane. Mammalian AQP8 has also been located to the inner mitochondrial membrane of rat hepatocytes (Calamita et al., 2005), where it is proposed to regulate mitochondrial water permeability. The present finding of salmon Aqp8aa(1+2) in the liver is strikingly similar to that reported in rat hepatocytes (Calamita et al., 2005), and seems to correspond to a mitochondrial or vesicular localization for this aquaporin. However, firm conclusions should await further examination by immunoelectron microscopy.

The brush border membrane localization of both Aqp8ab and -8b in the two salmonid species investigated here supports and extends the hypothesis of Tipsmark et al. (2010) and Madsen et al. (2011) that these aquaporins are important regulators of intestinal transepithelial water transport. The immunoelectron microscopy of Aqp8ab and Aqp8b in the rainbow trout intestine paralleled the findings by immunofluorescence in the intestine of Atlantic salmon. Unpublished observations from our laboratory using immunofluorescence or immunohistochemistry also show similar results in rainbow trout intestine with the Aqp8ab and -8b antibodies. Alignment of a known Aqp8ab from rainbow trout (Acc#CU071568) with the salmon Aqp8ab showed 100% identity at the antibody epitope and labeling with the Aqp8ab antibody is therefore likely a representative of a rainbow trout paralog. The antibody raised against Atlantic salmon Aqp8ab was developed based on EST data (Madsen et al., 2011). Due to a non-synonymous nucleotide polymorphism there is a single amino acid mismatch at the end of the epitope compared to the cloned paralog and the rainbow trout sequence (T in the antigenic peptide, P in the salmonid paralogs), however this does not seem to affect the binding of the antibody to the protein. There are currently no available EST data on rainbow trout Aqp8b, but based on the phylogenetic proximity of this species to the Atlantic salmon and the high similarity between Atlantic salmon and rainbow trout Aqp8aa and Aqp8ab proteins, we suspect that there is an Aqp8b paralog expressed in the intestine of rainbow trout with a similar

localization as observed for this paralog in Atlantic salmon. The intracellular localization of Aqp8b in the enterocytes and its presence in some goblet cells in the middle intestine suggest that different sorting mechanisms may exist for this and the Aqp8ab protein. Cross reactivity between the antibodies for the three different paralogs could be a valid concern, however control experiments using *X. laevis* oocytes showed that cross reactivity was minimal. Nevertheless, it cannot be excluded that the conformations of the proteins in the fixed intestine are such that cross reactivity might occur and yield false positive results. In addition, binding of primary antibodies to glycocalyx is sometimes mistaken as binding of the antibody to apical membrane proteins of intestinal epithelia or other mucous coated surfaces. However, the immunoelectron microscopy shows that binding of the antibodies to Aqp8ab and -8b in the apical membrane is indeed specific and not an artifact. The intestinal staining pattern of Aqp8ab and Aqp8b agree quite well with previously published results from the rat (Elkjær et al., 2001; Laforenza et al., 2005; Tritto et al., 2007) although the strongest staining in the small intestine of the rat with the AQP8 antibody was seen in the sub-apical part of the enterocytes rather than the brush border membrane found here in the salmon intestine. The immunoelectron microscopy also detected Aqp8ab and Aqp8b labeling in subapical vesicular structures. Whether Aqp8 proteins located in these vesicular structures are destined for plasma membrane insertion, degradation or recycling to other cellular compartments is presently unknown and requires closer investigation of marker proteins expressed in the vesicles associated with Aqp8 labeling. Different trafficking mechanisms may be responsible for recruiting the Aqp8 proteins to the intestinal brush border membrane. Trafficking may involve kinase phosphorylation of the proteins, and from this perspective it is interesting to note that Aqp8aa1 and -8b have predicted N-terminal serine phosphorylation residues that are missing in the Aqp8ab protein (*in silico* prediction using NetPhos 2.0; Blom et al., 1999). The role of these residues awaits further investigation.

Effect of seawater on protein expression of Aqp8ab and Aqp8b

The increasing intestinal expression of the Aqp8ab protein upon SW challenge supports previous reports of elevated *aqp8* mRNA levels in the intestine of various fish species exposed to SW (Cutler et al., 2009; Tipsmark et al., 2010, Kim et al., 2010). These findings underline the important role of this paralog in transforming the intestine into a water-absorptive organ when fish are exposed to hyperosmotic conditions. In this study, we analyzed protein expression in an enriched plasma membrane fraction, thus suggesting a functional membrane localization of Aqp8ab as observed by immunoelectron microscopy of Aqp8ab in the rainbow trout intestine. The immunoblots revealed

bands of higher and lower expected molecular weight than the native Aqp8 proteins. The nature of these bands are unknown at present but might reflect post translationally modified Aqp8 proteins (e.g. coupled to sugars, ubiquitin, etc.). As suggested by Madsen et al., (2011), apical as well as basolateral localization of Aqp8abmay create a regulated transcellular pathway of water movement, which may be supplemented by apical expression of other aquaporin paralogs - especially Aqp1aa (Martinez et al., 2005a, Raldúa et al., 2008, Madsen et al., 2011). Recent experiments using radiolabelled polyethylene glycol molecules in the intestine of killifish (*Fundulus heteroclitus*) have indeed shown that the transcellular route of water absorption is more important than the paracellular route (Wood & Grosell, 2012). Regulation of aquaporin expression in the intestine of fish upon SW challenge could thus prove valuable to the understanding of osmotic homeostasis in the intestine of vertebrates. In contrast to Aqp8ab, immunoblotting did not reveal any regulation of membrane bound Aqp8b protein or its mRNA upon SW transfer. This protein was localized apically, both in the brush border zone as well as sub-apically in vesicular compartments. The apparent lack of regulation and the ubiquitous tissue distribution suggests that Aqp8b performs a housekeeping function such as cell volume regulation or is associated with water homeostasis of intracellular compartments. A role in mucus secretion is also suggested by the presence of this paralog in goblet cells.

Conclusions and perspectives

In summary, we have characterized three main classes of Aqp8 in the Atlantic salmon. There appear to be yet more *aqp8* paralogs in the genome of Atlantic salmon as judged from the extra *aqp8aa* paralog which is consistent with the partial tetraploid status of this species. The paralogs investigated in the current study show divergent expression patterns, which suggests that they perform different functions in the tissues where they are expressed. Aqp8aa(1+2) is the main paralog expressed in the liver and may be involved in maintaining internal osmotic balance in hepatocytes or perhaps be involved in bile fluid formation, but the specific role of each paralog requires further investigation. Our data support a physiological role of Aqp8ab in the transcellular water uptake across intestinal enterocytes upon SW exposure where Aqp8b may play a supporting role. Goblet cell expression of Aqp8b suggests that this protein has a role in mucus production/secretion, as suggested for Aqp1aa (*S. salar* intestine: Madsen et al., 2011) and Aqp3b (*A. anguilla* rectum: Lignot et al., 2002; esophagus: Cutler et al., 2007). The acquired glycerol permeability of the Aqp8ab and Aqp8b paralogs and their distinct expression profiles suggest that

619 the Atlantic salmon Aqp8 water channels have neofunctionalized. In future studies it will be
620 important to decipher the hormonal and environmental factors that initiate the divergent expression
621 patterns and the structural alterations that facilitated a broader selection of solutes to permeate the
622 channel.
623
624 **Acknowledgements**
625 The staff at the Danish centre for Wild Salmon is thanked for their help with animal husbandry and
626 seawater challenge experiments. Annette Duus and Else-Merete Løcke are thanked for valuable
627 technical assistance. This study was supported by grants from the Danish Natural Research Council
628 (09-070689 to SSM), a Grant of the Spanish Ministry of Science and Innovation (MICINN;
629 AGL2010-15597) to J.C., and a Grant from the Research Council of Norway (204813) to R.N.F.
630 B.M.C. was supported by The Danish Council for Independent Research - Medical Sciences and the
631 Lundbeck Foundation and F.C. was supported by a postdoctoral contract Juan de la Cierva from
632 Spanish MICINN.
633

References

Ando, M., Mukuda, T., and Kozaka, T. (2003). Water metabolism in the eel acclimated to seawater: from mouth to intestine. *Comp. Biochem. Physiol. B* **136**, 621-633.

Beyenbach, K. (2004). Kidneys sans glomeruli. *Am. J. Physiol., Renal. Physiol.* **286**, F811-F827.

Blom, N., Gammeltoft, S., and Brunak, S. (1999). Sequence- and structure-based prediction of eukaryotic protein phosphorylation sites. *J. Mol. Biol.* **294**, 1351-1362.

Brown, J. A., Jackson, B. A., Oliver, J. A., and Henderson, I. W. (1978). Single nephron filtration rates (SNGFR) in the trout, *Salmo gairdneri. Pflügers Arch.* **377**, 101-108.

Brown J. A., Oliver J. A., Henderson I. W., and Jackson B. A. (1980). Angiotensin and single nephron glomerular function in the trout, *Salmo gairdneri. Am. J. Physiol., Regul. Integr. Comp. Physiol*. **239**, R509–R514.

Buddington, R. K., and Diamond, J. M. (1987). Pyloric ceca of fish: a "new" absorptive organ. *Am. J. Physiol., Gastrointestinal and Liver Physiol*. **252**, G65-G76.

Calamita G., Ferri, D., Gena, P., Liquori, G. E., Cavalier, A., Thomas, D., and Svelto, M. (2005). The Inner Mitochondrial Membrane Has Aquaporin-8 Water Channels and is Highly Permeable to Water. *J. Biol. Chem*. **280** (17), 17149-17153

Cerdà, J. and Finn, R. N. (2010). Piscine aquaporins: an overview of recent advances. *J. Exp. Zool*. **313A**, 1-28.

Cutler, C.P. and Cramb, G. (2002). Branchial expression of an aquaporin 3 (AQP-3) homologue is downregulated in the European eel (*Anguilla anguilla*) following seawater acclimation. *J. Exp. Biol.* **205,** 2643-2651.

Cutler, C.P., Martinez, A.S., and Cramb, G. (2007). The role of aquaporin 3 in teleost fish. *Comp. Biochem. Physiol.* **148A**, 82-91.

Cutler, C. P., Philips, C., Hazon, N., and Cramb, G. (2009). Aquaporin 8 (AQP8) intestinal mRNA expression increases in response to salinity acclimation in yellow and silver European eels (*Anguilla anguilla*). *Comp. Biochem. Physiol., Mol. Integr. Physiol.* **153A**, 78.

Davidson, W.S., Koop B. F., Jones, S. J. M., Iturra, P., Vidal, R., Maass, A., Jonassen, I., Lien, S., and Omholt, S. (2010). Sequencing the genome of the Atlantic salmon (*Salmo salar*). *Genome Biology* **11**, 403-409.

Deen, P. M. T., Verdijk, M. A. J., Knoers, N., Wieringa, B., Monnens, L. A., van Os, C. H., and van Oost, B. A. (1994). Requirement of human renal water channel aquaporin-2 for vasopressin-dependent concentration of urine. *Science* **264**, 92-95.

Elkjær, M. L., Nejsum, L. N., Grecz, V., Kwon, T. H., Jensen, U. B., Frøkiær, J., and Nielsen, S. (2001). Immunolocalization of aquaporin-8 in rat kidney, gastrointestinal tract, testis and airways. *Am. J. Physiol., Renal Physiol.* ***281***, F1047-F1057.

Engelund, M. B. and Madsen, S. S. (2011). The role of aquaporins in the kidney of euryhaline teleosts. *Front. Physiol* **2**, 51. doi: 10.3389/fphys.2011.00051

Evans, D. H., Piermarini, P. M., and Choe, K. P. (2005). The multifunctional fish gill: Dominant site of gas exchange, osmoregulation, acid-base regulation, and excretion of nitrogenous waste. *Physiol Rev* **85**, 97-177.

Fabra, M., Raldúa, D., Bozzo, M. G., Deen, P. M. T., Lubzens, E., and Cerdà, J. (2006). Yolk proteolysis and aquaporin-1o play essential roles to regulate fish oocyte hydration during meiosis resumption. *Develop. Biol.* **295**, 250-262.

Fabra, M., Raldúa, D., Power, D. M., Deen, P. M. T., and Cerdà, J. (2005). Marine fish egg hydration is aquaporin-mediated. *Science* **307**, 545.

Finn, R. N. and Cerdà, J. (2011). Aquaporin evolution in fishes. *Front. Physiol.* **2**, 44. doi: 10.3389/fphys.2011.00044.

García, F., Kierbel, A., Larocca, M. C., Gradilone, S. A., Splinter, P., LaRusso, N. F., and Marinelli, R. A. (2001). The Water Channel Aquaporin-8 Is Mainly Intracellular in Rat Hepatocytes, and Its Plasma Membrane Insertion Is Stimulated by Cyclic AMP. *J. Biol. Chem.* **276** (15), 12147-12152.

Grosell M, O'Donnell, M. J., Wood, C. M. (2000). Hepatic versus gallbladder bile composition: in vivo transport physiology of the gallbladder in rainbow trout. *Am. J. Physiol., Regul. Integr. Comp. Physiol.* **278**, R1674-R1684.

Hiroi, J., McCormick, S.D., Ohtani-Kaneko. R., and Kaneko, T. (2005). Functional classification of mitochondrion-rich cells in euryhaline Mozambique tilapia (Oreochromis mossambicus) embryos, by means of triple immunofluorescence staining for Na/K+-ATPase, Na+/K+/2Cl(-) cotransporter and CFTR anion channel. *J. Exp. Biol.* **208**, 2023-2036.

Hwang, P. P., Lee, T.H., and Lin, L. Y. (2011). Ion regulation in fish gills: recent progress in the cellular and molecular mechanisms. *Am. J. Physiol., Regul. Integr. Comp. Physiol*. **301**, R28-R47.

Kamsteeg, E. J. and Deen, P. M. (2001). Detection of aquaporin-2 in the plasma membranes of oocytes: a novel isolation method with improved yield and purity. *Biochem Biophys Res Commun.* **282**, 683-690.

Karnaky K. J. (1986). Structure and Function of the Chloride Cell of Fundulus-Heteroclitus and Other Teleosts. *Am. Zool.* **26**, 209-224.

Katoh, K. and Toh, H. (2008). Recent developments in the MAFFT multiple sequence alignment program. *Brief. Bioinform.* **9**, 286–298.

Kim, Y. K., Watanabe, S., Kaneko, T., Do Huh, M., and Park, S. I. (2010). Expression of aquaporins 3, 8 and 10 in the intestines of freshwater- and seawater-acclimated Japanese eels *Anguilla japonica*. *Fish. Sci.* ***76***, 695-702.

Laforenza, U., Cova, E., Gastaldi, G., Tritto, S., Grazioli, M., LaRusso, N. F., Splinter, P. L., D'Adamo, P., Tosco, M., and Ventura, U. (2005). Aquaporin-8 is involved in water transport in isolated superficial colonocytes from rat proximal colon. *J. Nutrit.* **135,** 2329-2336.

Lignot, J. H., Cutler, C. P., Hazon, N., and Cramb, G. (2002). Immunolocalisation of aquaporin 3 in the gill and the gastrointestinal tract of the European eel *Anguilla anguilla* (L.). *J. Exp. Biol.* **205**, 2653-2663.

Liu, K., Nagase, H., Huang, C. G., Calamita, G., and Agre, P. (2006). Purification and functional characterization of aquaporin-8. *Biol. Cell* **98**, 153-161

Ma, T., Yang, B., and Verkman, A. S. (1997). Cloning of a Novel Water and Urea-Permeable Aquaporin from Mouse Expressed Strongly in Colon, Placenta, Liver and Heart. *Biochemical and Biophysical Research Communications* **240**, 324-328.

Madsen, S. S., Olesen, J. H., Bedal, K., Engelund, M. B., Velasco-Santamaría, Y. M., and Tipsmark, C. K. (2011). Functional characterization of water transport and cellular localization of three aquaporin paralogs in the salmonid intestine. *Front. Physiol.* **2**, 56. doi: 10.3389/fphys.2011.00056

Martinez, A. S., Cutler, C. P., Wilson, G. D., Phillips, C., Hazon, N., and Cramb, G. (2005a). Regulation of expression of two aquaporin homologs in the intestine of the European eel: effects of seawater acclimation and cortisol treatment. *Am. J. Physiol., Regul. Integr. Comp. Physiol.* 288, R1733–R1743.

Martinez, A. S., Cutler, C. P., Wilson, G. D., Phillips, C., Hazon, N., and Cramb, G. (2005b). Cloning and expression of three aquaporin homologues from the European eel (*Anguilla anguilla*): effects of seawater acclimation and cortisol treatment on renal expression. *Biol. Cell* 97, 615-627.

McDonald, M. D. (2007). The renal contribution to salt and water balance. In *Fish Osmoregulation* (ed. B. Baldisserotto, J. M. M. Romero and B. G. Kapoor), pp. 322-345. Enfield, NH, USA: Science Publishers.

Moghadam, H.K., Ferguson, M.M., and Danzmann, R.G. (2011). Whole genome duplication: challenges and considerations associated with sequence orthology assignment in Salmoninae. *J. Fish Biol.* **79**, 561-574.

Notredame, C., Higgins, D.G., and Herringa, J. (2000). T-Coffee: a novel method for fast and accurate multiple sequence alignment. *J. Mol. Biol.* **302**, 205–217.

Olsvik, P. Å., Lie, K. K., Jordal, A. O., Nilsen, T. O., and Hordvik, I. (2005). Evaluation of potential reference genes in real-time RT-PCR studies of Atlantic salmon. *BMC Mol. Biol.* **6,** Art. 21.

Pfaffl M. W. (2001). A new mathematical model for relative quantification in real-time RT-PCR. *Nucleic Acids Res* **29**, e45.

Raldúa, D., Otero, D., Fabra, M., and Cerdà, J. (2008). Differential localization and regulation of two aquaporin-1 homologs in the intestinal epithelia of the marine teleost *Sparus aurata*. *Am. J. Physiol., Regul. Integr. Comp. Physiol.* **294**, R993-R1003.

Ronquist, F. and Huelsenbeck, J.P. (2003). MrBayes 3: Bayesian phylogenetic inference under mixed models. *Bioinformatics* **19**, 1572–1574.

Rozen, S. and Skaletsky, H. J. (2000). Primer3 on the WWW for general users and for biologist programmers. In *Bioinformatics Methods and Protocols: Methods in Molecular Biology* (e.d. S. Krawetz, and S. Misener), pp. 365-386. Totowa, NJ: Humana Press.

Saparov, S. M., Liu, K., Agre, P., and Pohl, P. (2007). Fast and Selective Ammonia Transport by Aquaporin-8. *J. Biol. Chem.* **282**, 5296-5301.

Smith, H. W. (1932). The absorption and excretion of water and salts by marine teleosts. *Q. Rev. Biol*. **7**, 1-26.

Sundell, K., Jutfelt, F., Ágústsson, T., Olsen, R., Sandblom, E., Hansen, T., and Björnsson, B. T. (2003). Intestinal transport mechanisms and plasma cortisol levels during normal and out-of-season parr-smolt transformation of Atlantic salmon, Salmo salar. *Aquaculture* **222**, 265-285.

Sundell, K. S. and Sundh, H. (2012). Intestinal fluid absorption in anadromous salmonids: importance of tight junctions and aquaporins. *Front. Physiol*. **3**:388. doi: 10.3389/fphys. 2012.00388

Suyama, M., Torrents, D. and Bork, P. (2006). PAL2NAL: robust conversion of protein sequence alignments into the corresponding codon alignments. *Nucleic Acids Res*. **34**, W609–W612.

Swafford, D.L. (2002). PAUP*. Phylogenetic analysis using parsimony (*and other models). Version 4.0b10 for macintosh. Sinauer Associates Inc, Sunderland, Mass.

Tingaud-Sequeira, A., Calusinska, M., Finn, R. N., Chauvigné, F., Lozano, J., and Cerdà, J. (2010). The zebrafish genome encodes the largest vertebrate repertoire of functional aquaporins with dual paralogy and substrate specificities similar to mammals. *BMC Evol. Biol*. **10**, 38

Tipsmark, C. K., Kiilerich, P., Nilsen, T. O., Ebbesson, L. O. E., Stefansson, S.O., and Madsen S. S. (2008). Branchial expression patterns of claudin isoforms in Atlantic salmon during seawater acclimation and smoltification. *Am. J. Physiol., Regul. Integr. Comp. Physiol*. **294**, R1563-R1574.

Tipsmark, C. K., Sørensen, K. J., and Madsen, S. S. (2010). Aquaporin expression dynamics in osmoregulatory tissues of Atlantic salmon during smoltification and seawater acclimation. *J. Exp. Biol*. **213**, 368-379.

Tritto, S., Gastaldi, G., Zelenin, S., Grazioli, M., Orsenigo, M. N., Ventura, U., Laforenza, U., and Zelenina, M. (2007). Osmotic water permeability of rat intestinal brush border membrane

vesicles: involvement of aquaporin-7 and aquaporin-8 and effect of metal ions. *Biochem. Cell Biol.* **85** *(6)*, 675-684.

Usher, M. L., Talbot, C., and Eddy, F. B. (1988). Drinking in Atlantic Salmon Smolts Transferred to Seawater and the Relationship Between Drinking and Feeding. *Aquaculture* **73**, 237-246.

Wood, C. M. and Grosell, M. (2012). Independence of net water flux from paracellular permeability in the intestine of *Fundulus heteroclitus*, a euryhaline teleost. *J. Exp. Biol*. **215**, 508-517.

Yang, B., Zhao, D., Solenov, E. and Verkman, A. S. (2006). Evidence from knockout mice against physiologically significant aquaporin 8-facilitated ammonia transport. *Am. J. Physiol*, *Cell. Physiol*. **291**, C417-C423.

Zapater, C., Chauvigné, F., Fernández-Gómez, B., Finn, R.N., and Cerdà, J. (2013). Alternative splicing of the nuclear progestin receptor in a perciform teleost generates novel mechanisms of dominant-negative transcriptional regulation. *Gen. Comp. Endocrinol.* **182**, 24-40.

Zapater, C., Chauvigné, F., Norberg, B., Finn, R.N., and Cerdà, J. (2011). Dual Neofunctionalization of a rapidly evolving aquaporin-1 paralog resulted in constrained and relaxed traits controlling channel function during meiosis resumption in teleosts. *Mol. Biol. Evol.* **28**, 3151-3169.

Figure Legends.

Figure 1. Molecular phylogeny of Atlantic salmon Aqp8 paralogs. (A) Bayesian majority rule consensus tree of the codon alignment. The tree is midpoint rooted. Posterior probabilities derived from 5 million MCMC generations of the codon/amino acid alignments are shown at each node. Scale bar represents the rate of nucleotide substitution per site. (B) Multiple sequence alignment of the Atlantic salmon (Ss) and zebrafish (Dr) Aqp8 paralogs highlighting the N-termini (NT), the five loops (A-E), the helical domains (H1-8), and the C-termini (CT). Fully conserved residues are boxed and shaded dark grey, while residues with similar chemical properties are shaded in light grey.

Figure 2. (A) Immunofluorescence micrographs of *X. laevis* oocytes expressing salmon aquaporin 8 paralogs and a noninjected control oocyte probed with one of the salmon Aqp antibodies (representative image). Size bars are 50 µm. B) Relative permeability to water (left panel), urea and glycerol (right panel) of *X. laevis* oocytes expressing salmon aquaporin 8 paralogs. Left: Noninjected oocytes or oocytes injected with cRNA corresponding to Aqp8aa1, Aqp8ab or Aqp8b subjected to swelling assays without further treatment (Ctrl) or subjected to 0.1mM HgCl (Hg) and in some cases followed by 5 mM β-mercaptoethanol to test for recovery prior to swelling assay. Asterisk indicate significant difference in relative water permeability between non injected and Ctrl oocytes ***: $P<0.001$. Right: Radioactive uptake of [^{3}H] glycerol or [^{14}C] urea by water injected oocytes or oocytes injected with cRNA as explained above. Asterisk indicate significant difference from water injected oocytes **: $P<0.01$, ***: $P<0.001$. Presented data is from one representative experiment and shown as mean ± SEM, N=12-20. C) Immunoblots of membrane fractions from *X. laevis* oocytes expressing Aqp8aa1, Aqp8ab or Aqp8b. Each antibody was probed against an enriched membrane fraction from oocytes expressing one of the three salmon aquaporin 8 paralogs or from control (C) oocytes. Molecular weight marker is shown on the left side.

Figure 3. (A,C,E) Tissue mRNA expression patterns of three Atlantic salmon *aqp8* paralogs. Tissues are shown in (E). mRNA expression is measured relative to *ef1a* and shown as mean ± SEM. N = 4, representing two SW acclimated and two FW acclimated salmon. n.d.: Not detected. Different letters indicate significant differences between tissue expression levels in each panel ($P<0.05$). (B) Immunoblots of membrane fractions from pyloric caeca of 7 days SW-acclimated

880 salmon (a and d) and 7 day sham transferred FW salmon (b and c) probed with antibodies against
881 Aqp8ab (a and b) or Aqp8b (c and d). Arrows point to native Aqp protein bands. Molecular weight
882 marker is shown on the left side. (D,F) mRNA expression patterns in relation to osmotic
883 environment of *aqp8ab* and *-8b* in intestinal tissue and spleen (shown in F). FW: freshwater, SW:
884 seawater, PC: pyloric caeca, MI: middle intestine, PI: posterior intestine, Spl.: spleen. Data is shown
885 as the mean value (N = 2).
886
887 Figure 4. Immunofluorescence micrographs of salmon aquaporin 8 paralogs in SW-acclimated
888 salmon. (A) Aqp8aa(1+2) (green) and the alpha subunit of the Na^+, K^+, ATPase (red) in middle
889 intestine. Inset: sub-apical localization of Aqp8aa(1+2). Asterisk in (A) and inset show enlarged
890 area and arrowhead point to approximate localization of the brush border. (B) Aqp8aa(1+2) (green)
891 in hepatic tissue, nuclei are counterstained with DAPI (blue). (C,F,I) pre-immune serum (green) for
892 Aqp8aa(1+2) (C), Aqp8ab (F) and Aqp8b (I) and the alpha subunit of the Na^+, K^+, ATPase (red) in
893 middle intestine. (D,E,G,H) Aqp8ab (D,E) (green) and Aqp8b (G,H) (green) and the alpha subunit
894 of the Na^+, K^+, ATPase (red) in middle intestine (D,G) and posterior intestine (E,H). Short arrows
895 in A and B point to intracellular vesicles. Long open arrows in D,E,G,H mark goblet cells and
896 arrowheads point to the brush border membrane of the intestinal epithelium. Size bars are 50 µm
897 except B where it is 25 µm.
898
899 Figure 5. Immunoelectron micrographs of Aqp8ab (A,B) and Aqp8b (C,D) in the middle intestine
900 of rainbow trout. (A and C) Both Aqp8ab and Aqp8b are abundantly expressed in the apical plasma
901 membrane (brush border) of enterocytes (arrows). (B and D) Expression of Aqp8ab and Aqp8b is
902 also seen in intracellular vesicles located subapically in the cell (arrowheads). Size bars are 0.5 µm.
903
904 Figure 6. The effect of SW-transfer on Aqp8ab (A,C) and Aqp8b (B,D) protein expression in
905 pyloric caeca (top panels) and middle intestine (lower panels) membrane fractions. Data are
906 normalized with respect to expression levels of β-actin proteins. Open squares represent SW-
907 transferred fish and closed circles represent sham transferred fish. Significant interaction between
908 time and treatment are indicated by ***SW x time ($P<0.001$). *** above data points show
909 significant difference between SW and sham transferred fish at that time point ($P<0.001$). Data are
910 shown as means ± SEM, N = 4-6. (E,F) Representative immunoblots of membrane fractions from
911 pyloric caeca of SW acclimated and sham transferred salmon. The blots were probed with

antibodies against Atlantic salmon Aqp8ab (E) or Aqp8b (F). Arrows point to protein bands used for the semi quantitative analysis in A-D.

914 Table 1. Primers used for cloning and QPCR of salmon aquaporin 8 paralogs

915 Primer	Primer sequence 5'→3'	Amplicon size
916 8aa1OFP	GTAAGTGACACAGAGAGCAGCAGTA	832 bp.
917 8aa1ORP	GTAAGTGACACAGAGAGCAGCAGTA	
918 8aa1CFP	ACT*AGATCT***ATG**TCTGTGATAGAGTCAAAGAC	816 bp.
919 8aa1CRP	AGC*GATATC***TTA**CTTCAGAACAAGACGTGTCT	
920 8abCFP	ACT*AGATCT***ATG**GGAGTTGAGAAAATGGAGCT	798 bp.
921 8abCRP	CGC*GATATC***TCA**CTTCATGATGATTCGTGTCTT	
922 8bbOFP	TCTCTCCAAACTCCTTTCCA	858 bp.
923 8bbORP	TGGCACTGCATGTAACAACA	
924 8bbCFP	ACT*AGATCT***ATG**ACAGAAGGGACAATGGAAC	798 bp.
925 8bbCRP	CGC*GATATC***TTA**CTTCATGAGAATACGTGTCTT	
926 8aa(1+2)QPCRFP*	TCATGACCCTCTTCCTGTCC	145 bp.
927 8aa(1+2)QPCRRP*	GGGTTCATACACCCTCCAGA	
928 8abQPCRFP*	GGAGCTGCCATGTCAAAGAT	159 bp.
929 8abQPCRRP*	CGCCCCTAGCAATACTACCA	
930 8bQPCRFP2 3UTR	GACACGCCTGCTCATTCG	71 bp.
931 8bQPCRRP2 3UTR	GTCTCCACCACCATTCAACAA	

932 Primers for aquaporin paralogs were constructed using the following EST's: *aqp8aa(1+2)*: CU071487 and DW573347,
933 *aqp8ab*: Ssa.15811 (formerly annotated as AQP-8b), *aqp8b*: ACN11279. *: Primers previously published (Tipsmark et
934 al., 2010). **Bold** marks start and stop codons. *Italic* marks BglII and EcoRV restriction sites. O(F/R)P: Primers
935 annealing outside coding sequence, used for nested PCR. C(F/R)P: Primers used for cloning of the full cDNA sequence.
936
937

Figure 1.

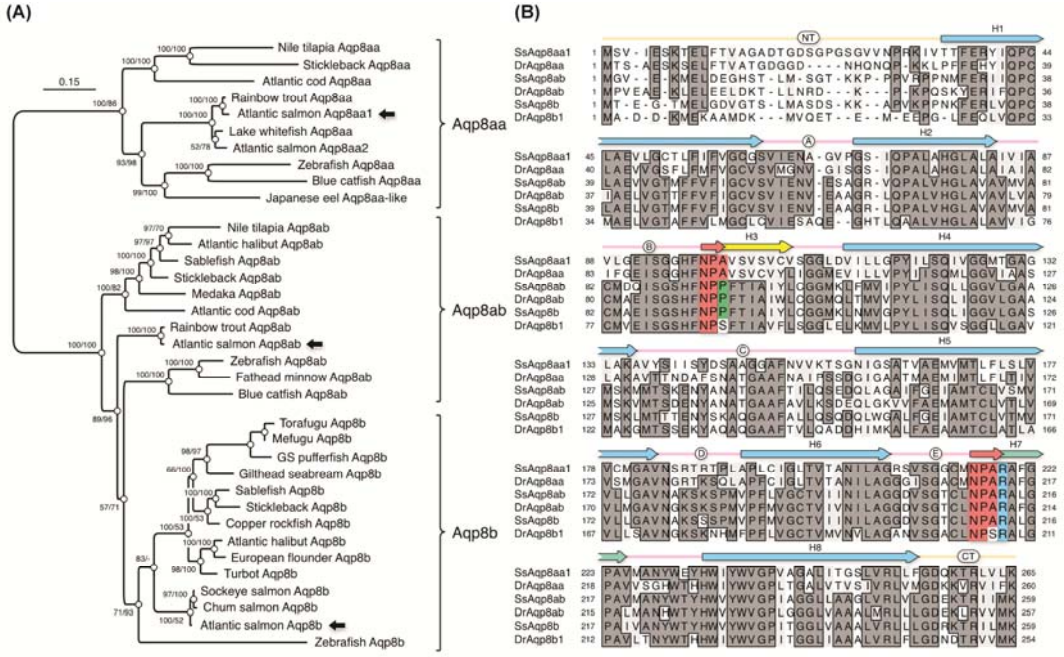

942 Figure 2.

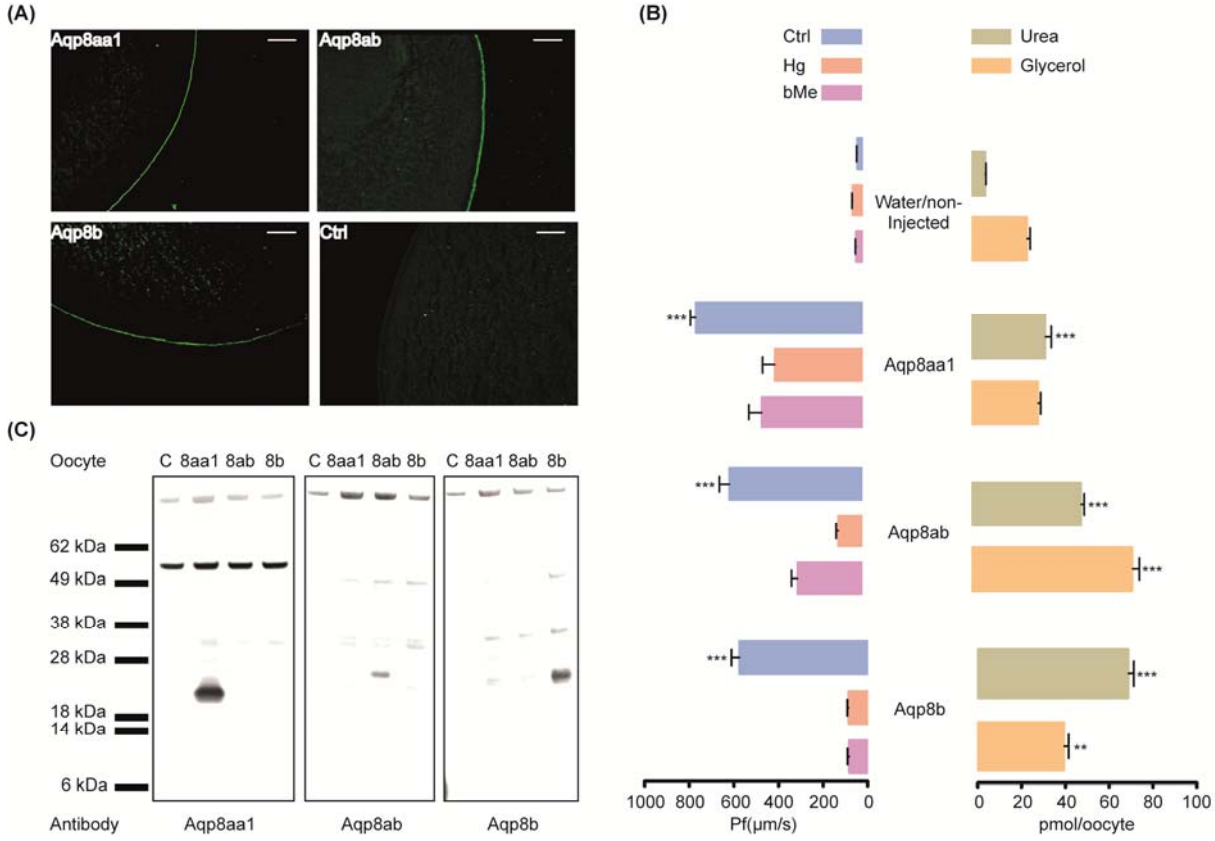

943

944

945 Figure 3.

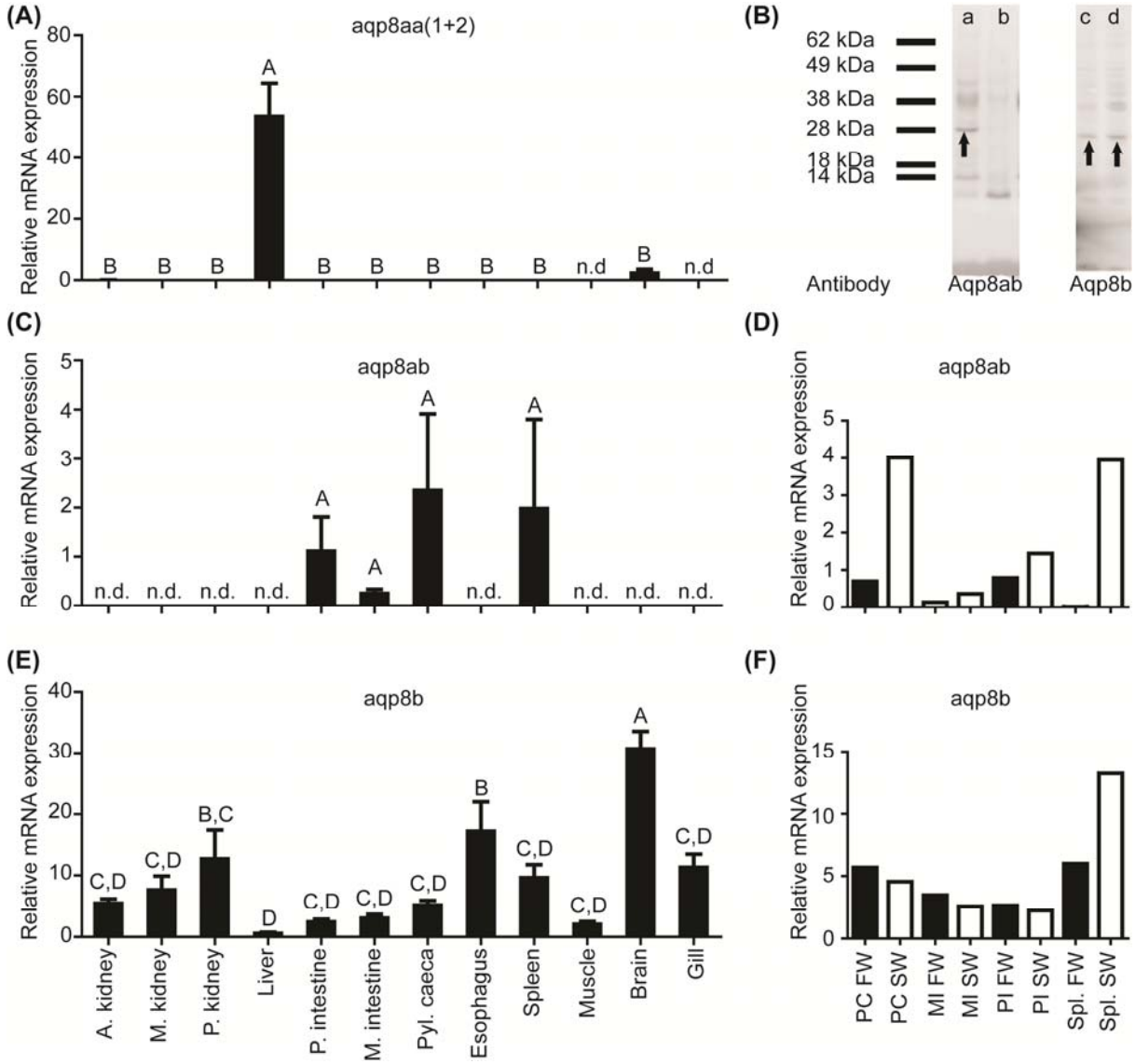

946

947

948

949 Figure 4.

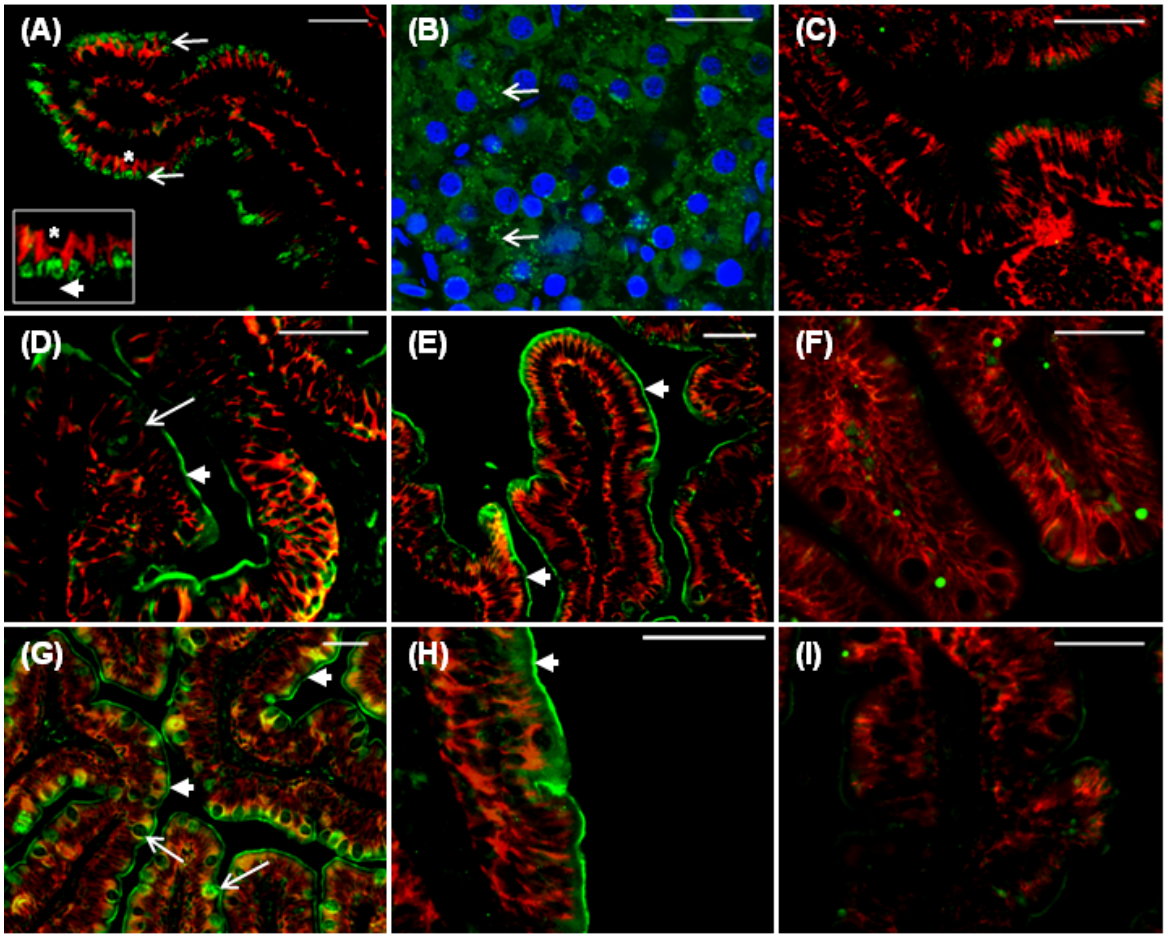

950

951 Figure 5.

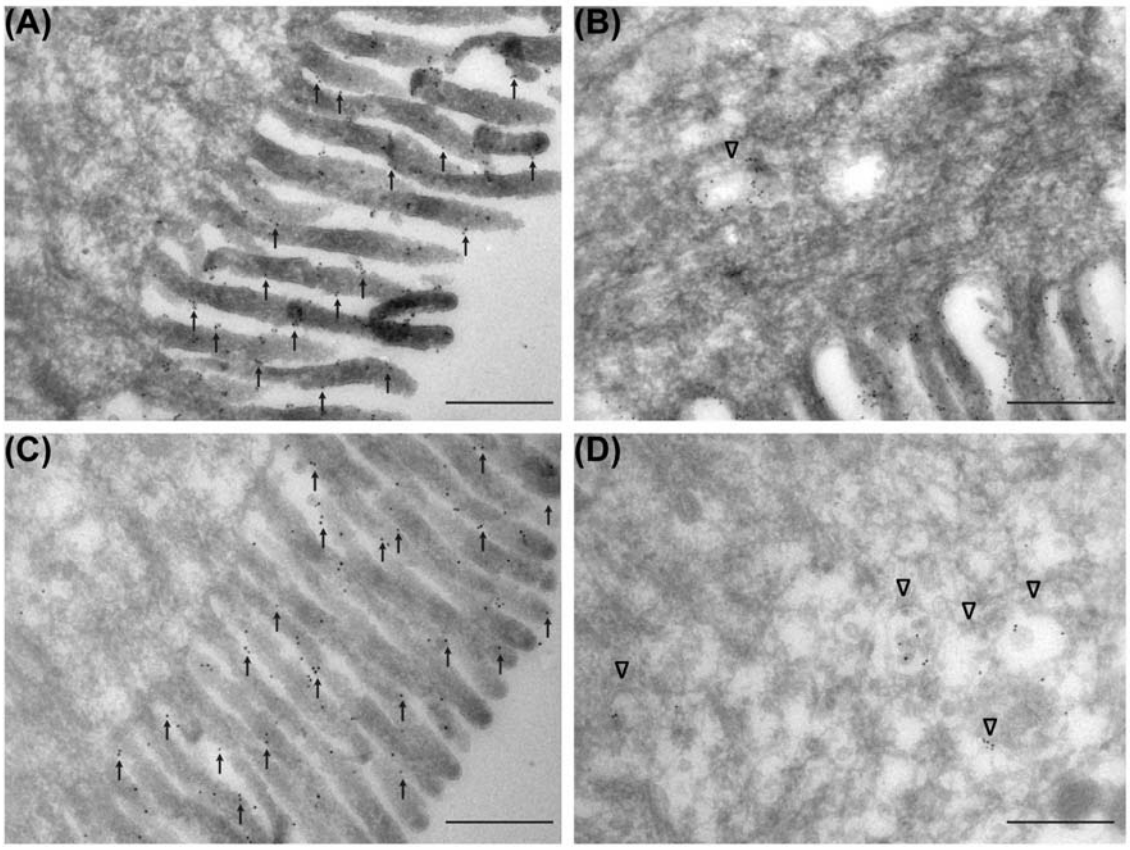

952

953

954 Figure 6.

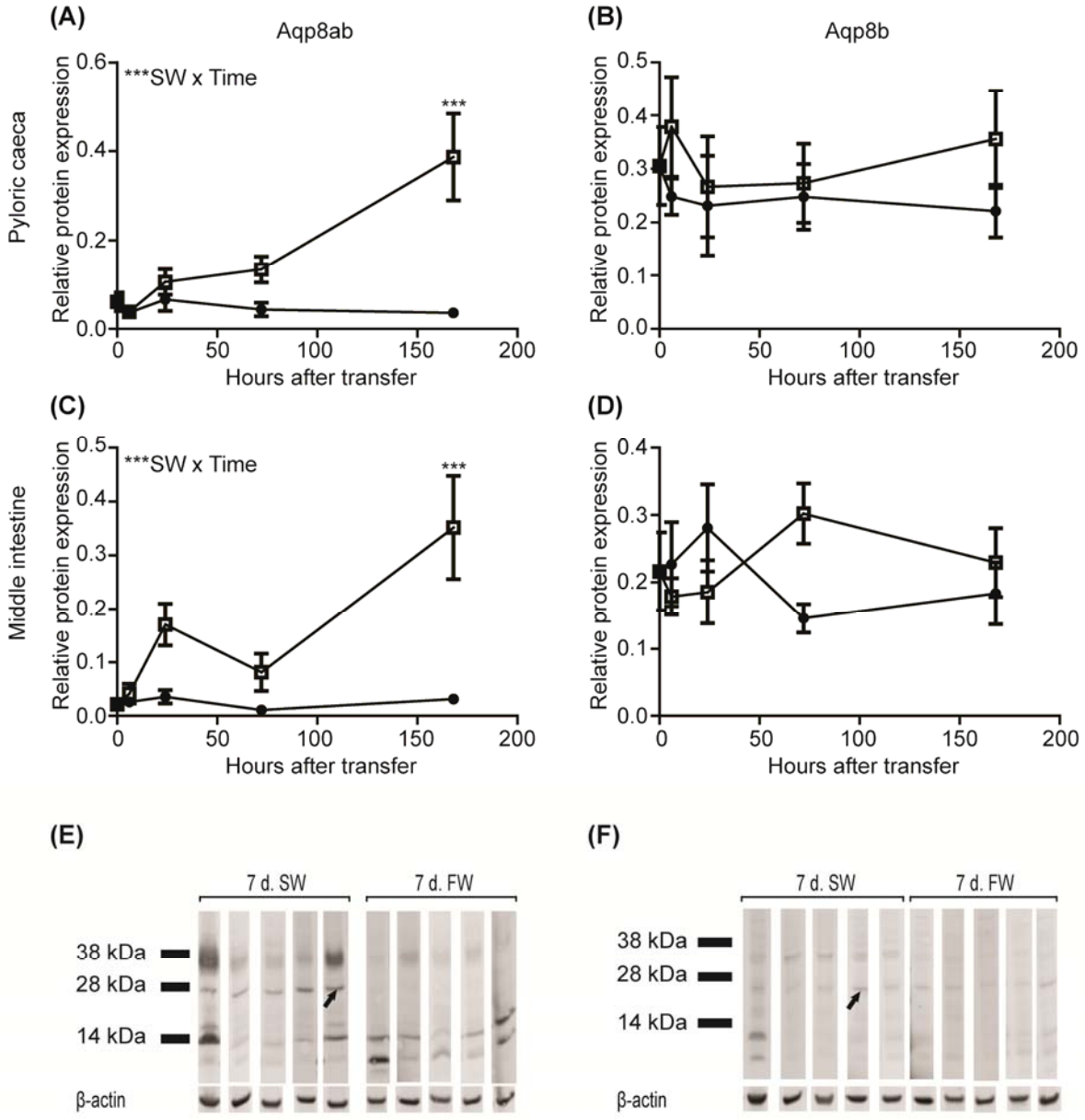

955

956

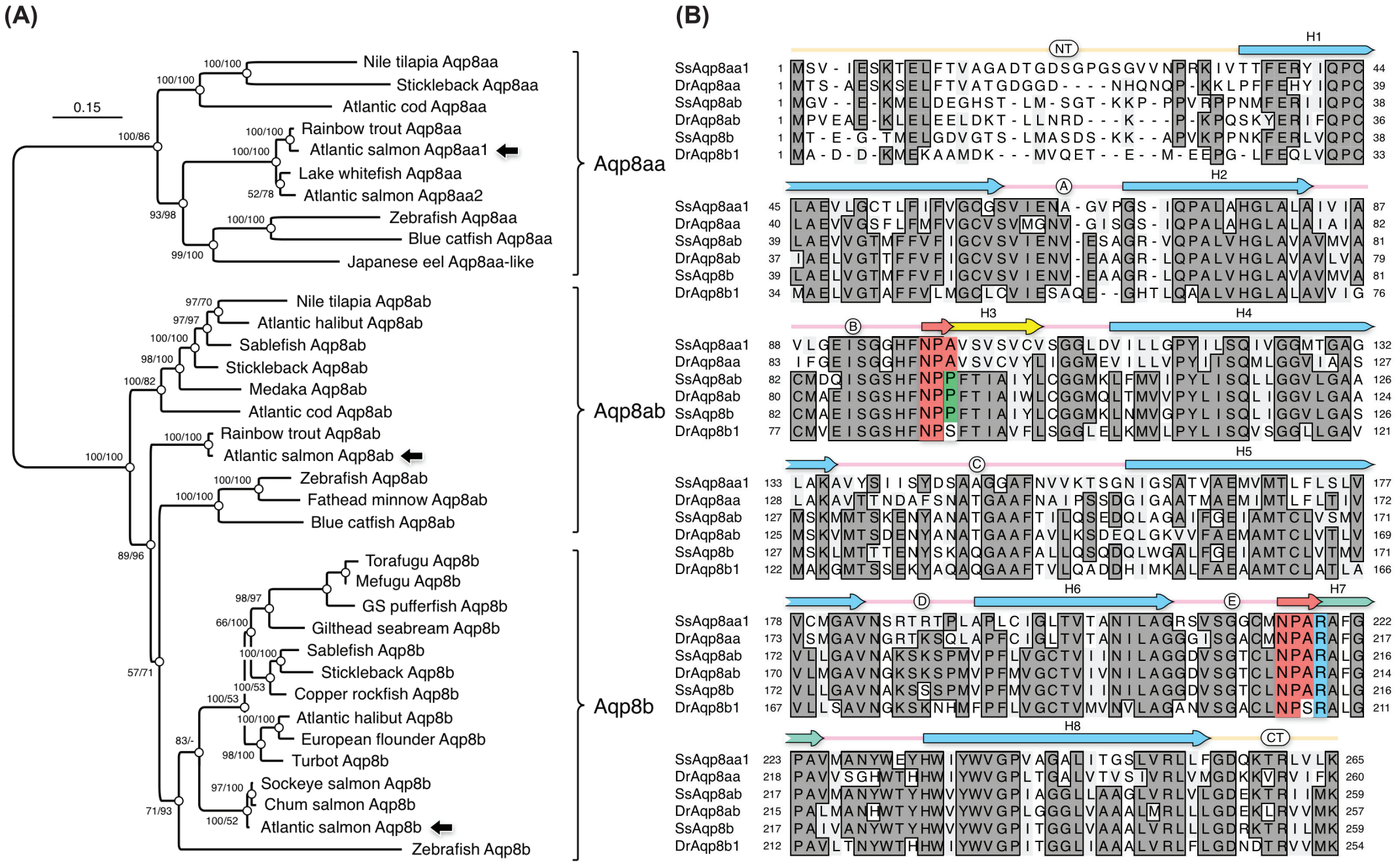
(A)
0.15
Nile tilapia Aqp8aa
Stickleback Aqp8aa
Atlantic cod Aqp8aa
Rainbow trout Aqp8aa
Atlantic salmon Aqp8aa1
Lake whitefish Aqp8aa
Atlantic salmon Aqp8aa2
Zebrafish Aqp8aa
Blue catfish Aqp8aa
Japanese eel Aqp8aa-like
Aqp8aa
Nile tilapia Aqp8ab
Atlantic halibut Aqp8ab
Sablefish Aqp8ab
Stickleback Aqp8ab
Medaka Aqp8ab
Atlantic cod Aqp8ab
Rainbow trout Aqp8ab
Atlantic salmon Aqp8ab
Zebrafish Aqp8ab
Fathead minnow Aqp8ab
Blue catfish Aqp8ab
Aqp8ab
Torafugu Aqp8b
Mefugu Aqp8b
GS pufferfish Aqp8b
Gilthead seabream Aqp8b
Sablefish Aqp8b
Stickleback Aqp8b
Copper rockfish Aqp8b
Atlantic halibut Aqp8b
European flounder Aqp8b
Turbot Aqp8b
Sockeye salmon Aqp8b
Chum salmon Aqp8b
Atlantic salmon Aqp8b
Zebrafish Aqp8b
Aqp8b
(B)
NT
H1
H2
H3
H4
H5
H6
H7
H8
CT
SsAqp8aa1
DrAqp8aa
SsAqp8ab
DrAqp8ab
SsAqp8b
DrAqp8b1

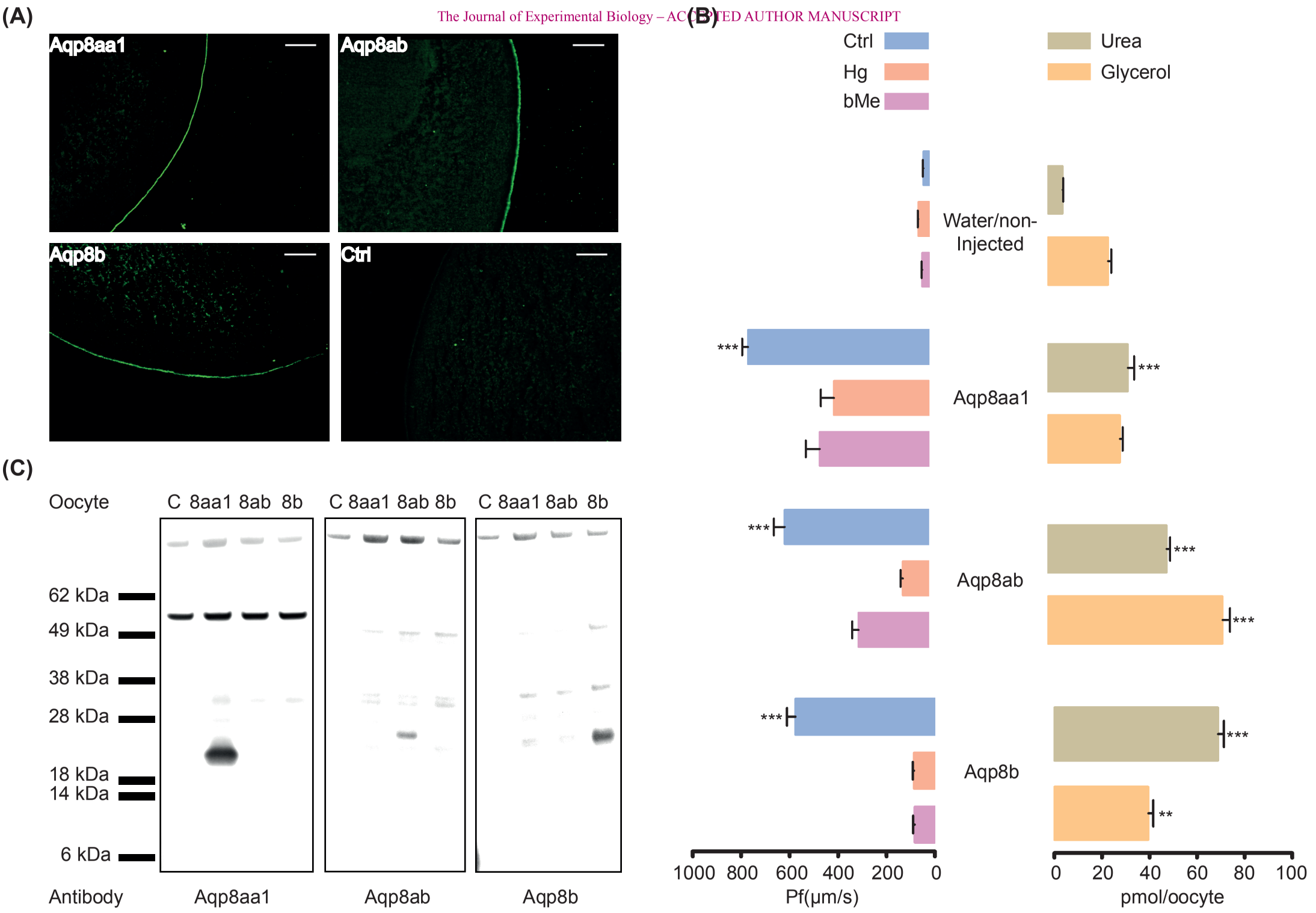
(A)
Aqp8aa1
Aqp8ab
Aqp8b
Ctrl
(B)
Ctrl
Hg
bMe
Urea
Glycerol
Water/non-Injected
Aqp8aa1
Aqp8ab
Aqp8b
***
**
1000 800 600 400 200 0
Pf(μm/s)
0 20 40 60 80 100
pmol/oocyte
(C)
Oocyte
C 8aa1 8ab 8b
62 kDa
49 kDa
38 kDa
28 kDa
18 kDa
14 kDa
6 kDa
Antibody
Aqp8aa1
Aqp8ab
Aqp8b

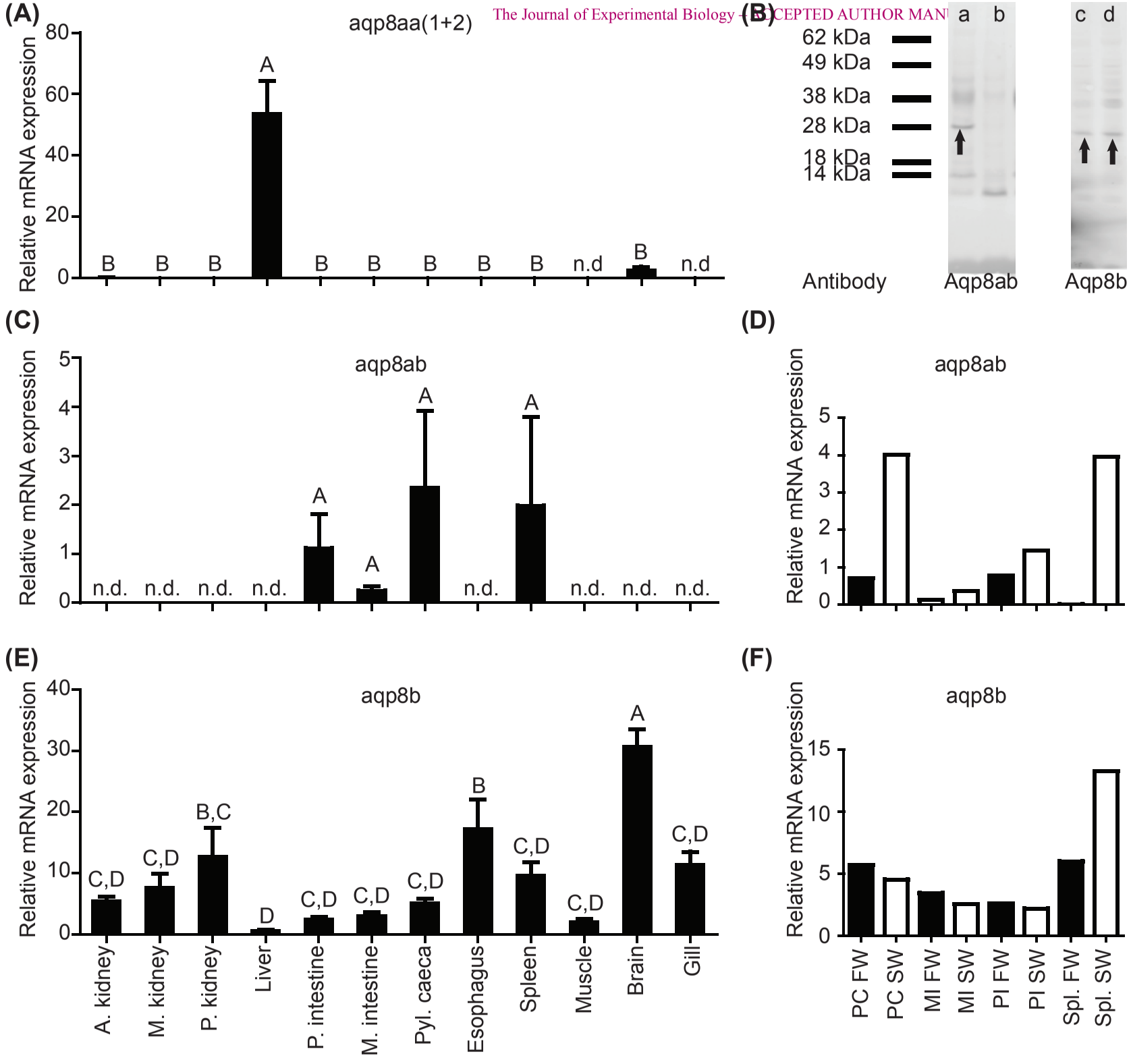

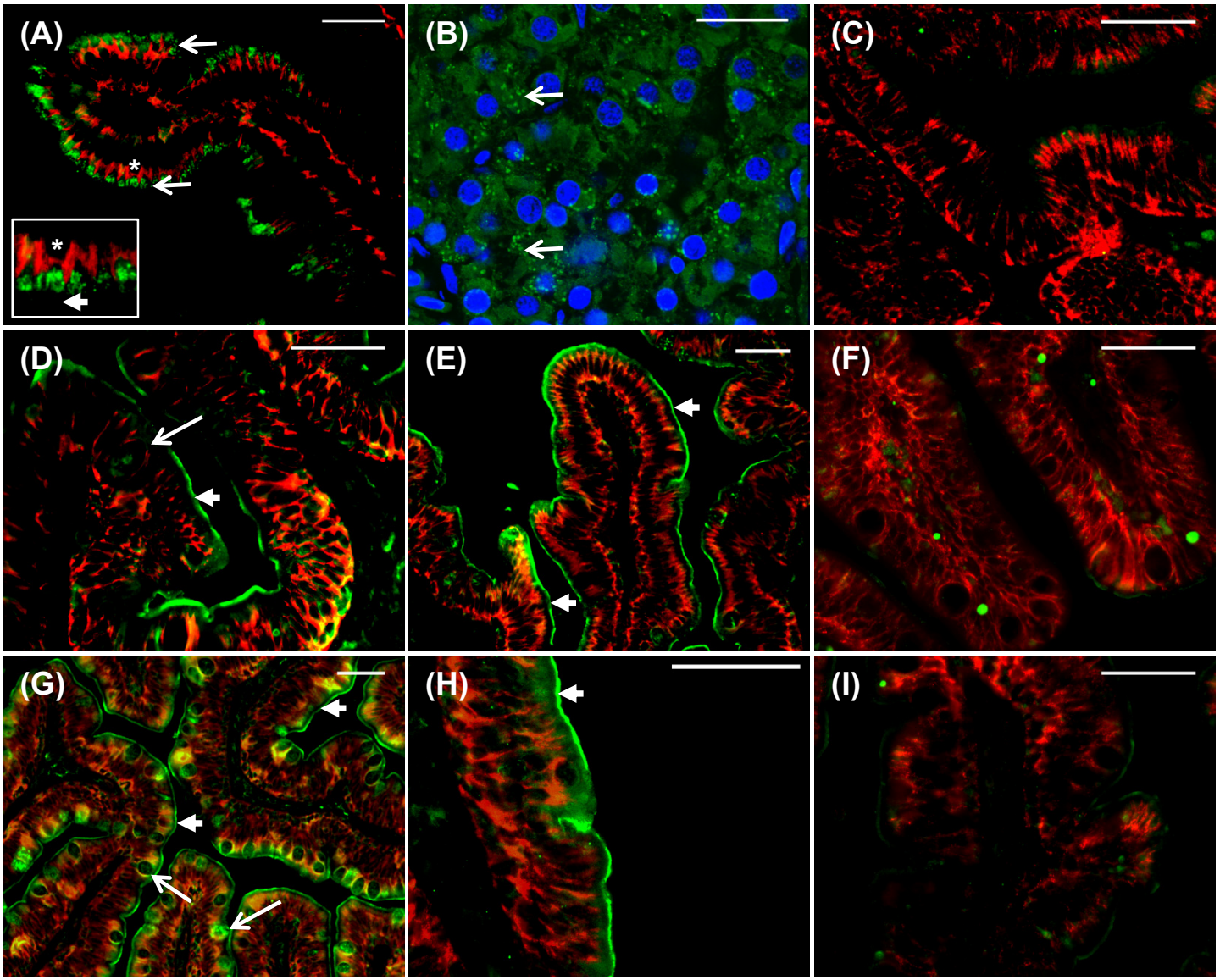

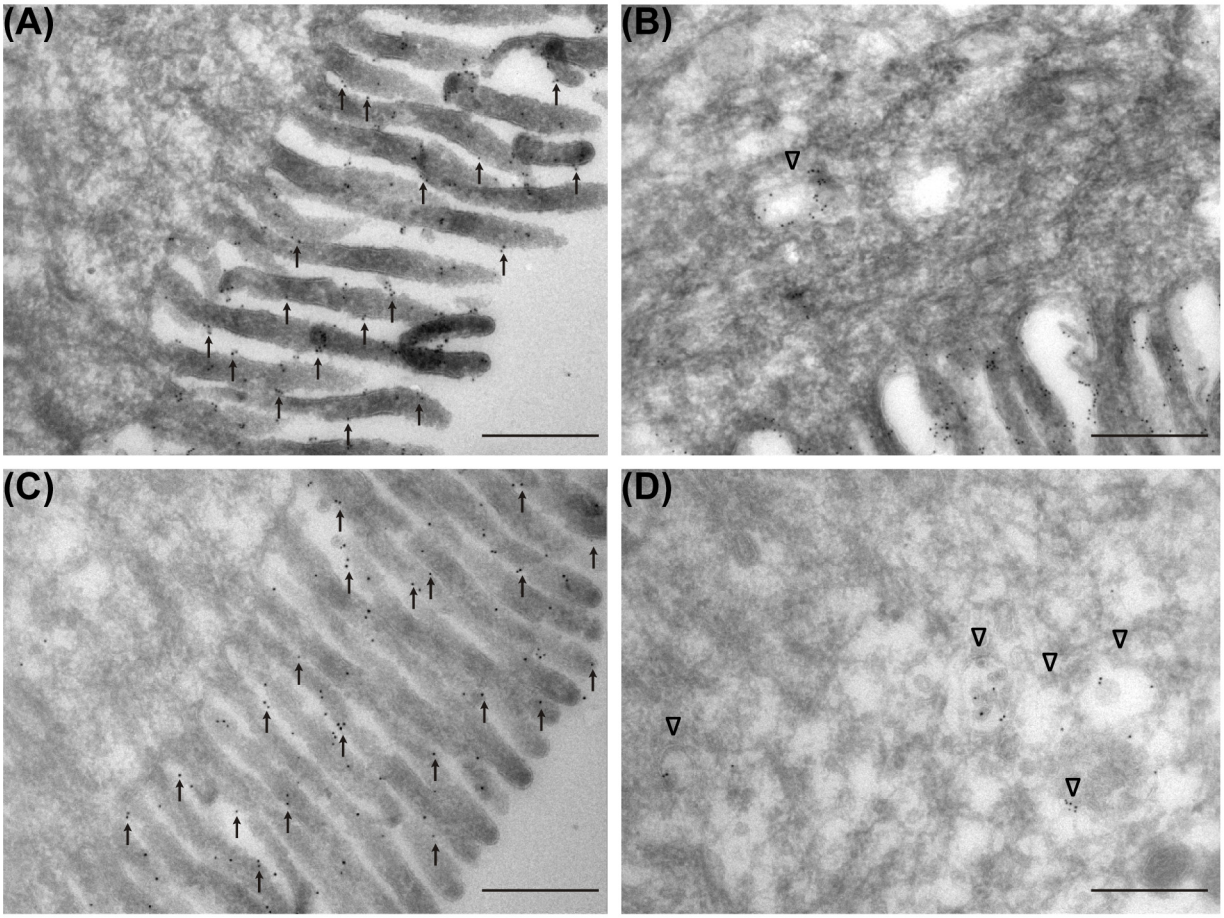

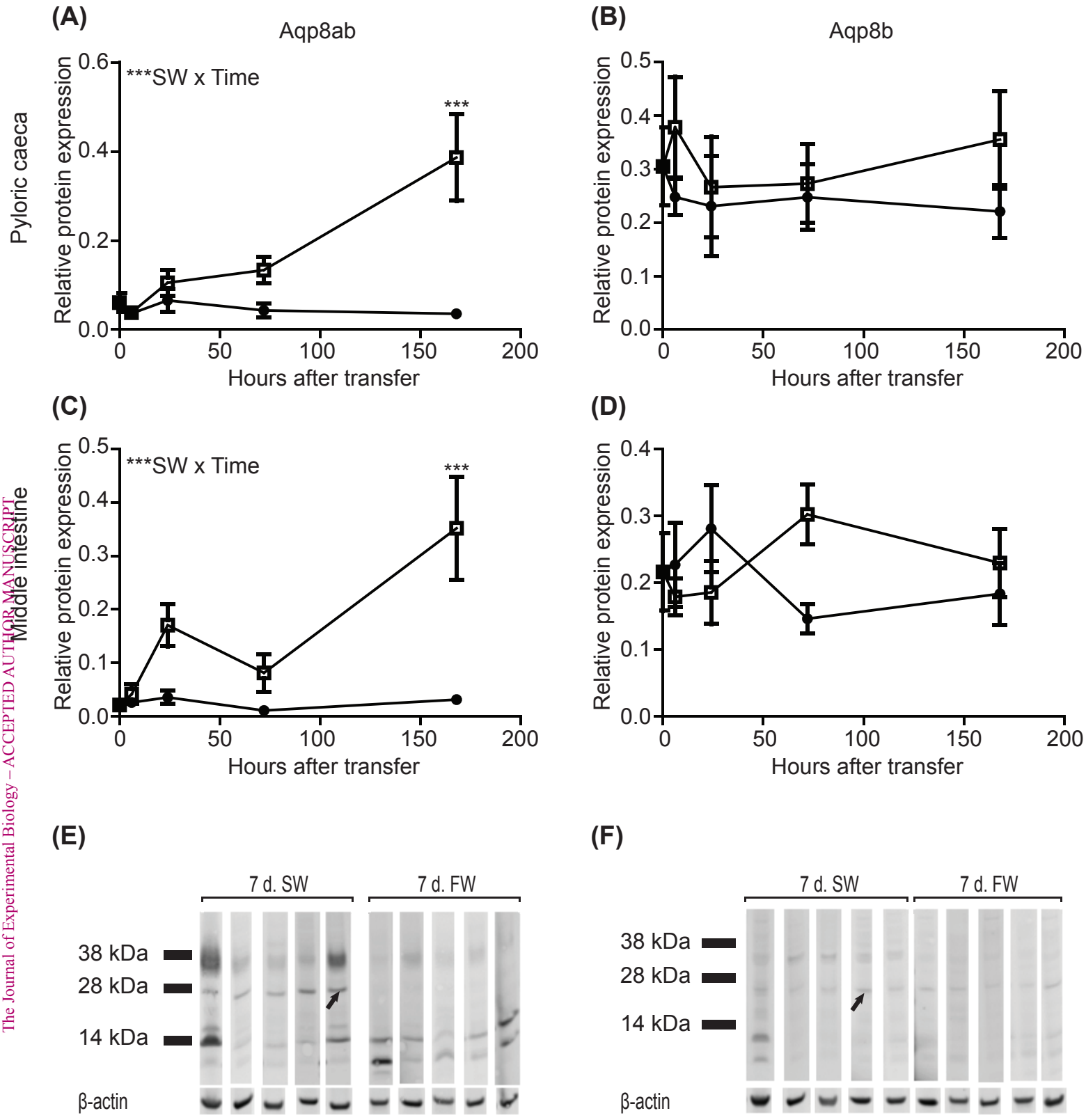

Table 1. Primers used for cloning and QPCR of salmon aquaporin 8 paralogs

Primer	Primer sequence 5'→3'	Amplicon size
8aa1OFP	GTAAGTGACACAGAGAGCAGCAGTA	832 bp.
8aa1ORP	GTAAGTGACACAGAGAGCAGCAGTA	
8aa1CFP	ACT*AGATCT***ATG**TCTGTGATAGAGTCAAAGAC	816 bp.
8aa1CRP	AGC*GATATC***TTA**CTTCAGAACAAGACGTGTCT	
8abCFP	ACT*AGATCT***ATG**GGAGTTGAGAAAATGGAGCT	798 bp.
8abCRP	CGC*GATATC***TCA**CTTCATGATGATTCGTGTCTT	
8bbOFP	TCTCTCCAAACTCCTTTCCA	858 bp.
8bbORP	TGGCACTGCATGTAACAACA	
8bbCFP	ACT*AGATCT***ATG**ACAGAAGGGACAATGGAAC	798 bp.
8bbCRP	CGC*GATATC***TTA**CTTCATGAGAATACGTGTCTT	
8aa(1+2)QPCRFP*	TCATGACCCTCTTCCTGTCC	145 bp.
8aa(1+2)QPCRRP*	GGGTTCATACACCCTCCAGA	
8abQPCRFP*	GGAGCTGCCATGTCAAAGAT	159 bp.
8abQPCRRP*	CGCCCCTAGCAATACTACCA	
8bQPCRFP2 3UTR	GACACGCCTGCTCATTCG	71 bp.
8bQPCRRP2 3UTR	GTCTCCACCACCATTCAACAA	

Primers for aquaporin paralogs were constructed using the following EST's: *aqp8aa(1+2)*: CU071487 and DW573347, *aqp8ab*: Ssa.15811 (formerly annotated as AQP-8b), *aqp8b*: ACN11279. *: Primers previously published (Tipsmark et al., 2010). **Bold** marks start and stop codons. *Italic* marks BglII and EcoRV restriction sites. O(F/R)P: Primers annealing outside coding sequence, used for nested PCR. C(F/R)P: Primers used for cloning of the full cDNA sequence.